CELL BIOLOGY

Platelet P-selectin initiates cross-presentation and dendritic cell differentiation in blood monocytes

Patrick Han[1]*, Douglas Hanlon[2]*, Najla Arshad[3], Jung Seok Lee[4], Kazuki Tatsuno[2], Eve Robinson[2], Renata Filler[2], Olga Sobolev[2], Christine Cote[5], Felix Rivera-Molina[6], Derek Toomre[6], Tarek Fahmy[1,2,3,4†], Richard Edelson[2†]

Dendritic cells (DCs) are adept at cross-presentation and initiation of antigen-specific immunity. Clinically, however, DCs produced by in vitro differentiation of monocytes in the presence of exogenous cytokines have been met with limited success. We hypothesized that DCs produced in a physiological manner may be more effective and found that platelets activate a cross-presentation program in peripheral blood monocytes with rapid (18 hours) maturation into physiological DCs (phDCs). Differentiation of monocytes into phDCs was concomitant with the formation of an "adhesion synapse," a biophysical junction enriched with platelet P-selectin and monocyte P-selectin glycoprotein ligand 1, followed by intracellular calcium fluxing and nuclear localization of nuclear factor κB. phDCs were more efficient than cytokine-derived DCs in generating tumor-specific T cell immunity. Our findings demonstrate that platelets mediate a cytokine-independent, physiologic maturation of DC and suggest a novel strategy for DC-based immunotherapies.

INTRODUCTION

Dendritic cells (DCs), termed "professional" antigen-presenting cells (APCs) for their capacity to process and cross-present antigens for induction of potent antigen-specific T cell responses, are principal regulators of adaptive immunity (*1*). However, naturally occurring DC populations in the blood, i.e., "BDCA$^+$ classical DC" (cDC), are rare, composing <1% of circulating leukocytes (*2*). Therefore, acquisition of large numbers of DCs for research and immunotherapeutic purposes typically involves ex vivo conversion of blood monocytes via cultivation with supraphysiologic concentrations of cytokines, including granulocyte-macrophage colony-stimulating factor (GM-CSF) and interleukin-4 (IL-4) (*3*) for up to 7 days.

While ex vivo–generated cytokine-derived DCs have offered enormous insights into the function of these cells, their relationship to DC populations arising in vivo is still poorly understood (*4*). Cytokine-derived DC and cDC share key genetic profiles for antigen processing and costimulation (*5*) but have been shown to be functionally distinct, especially in their induction of effector responses in vitro (*6*) and in vivo (*7*). Notably, as immunotherapies using cytokine-derived DCs have been met with disappointing clinical outcomes (*8*), the biologic integrity of ex vivo cytokine maturation has been questioned even by the originators of this methodology (*9*). Current hypotheses attribute these therapeutic dysfunctions to a combination of factors, namely, restricted life cycle and migration to the draining lymph nodes (*8*), loss of responsiveness and "exhaustion" against in vivo cytokine cues (*10*), and limited capacity for effector activation (*11*), implicating the production method of cytokine-derived DCs for shortcomings concerning physiologic performance in vivo.

In contrast to long-term, high-concentration cytokine cultures, rapid acquisition of DC-like features has been demonstrated in blood monocytes in the presence of inflammatory stimuli (*12*) through GM-CSF–independent (*13*) mechanisms in vivo, indicating the potentials for more "physiological" pathways of DC biogenesis. The case for using noncytokine cues to drive DC differentiation is bolstered when considering work that demonstrates inflammatory events such as extravasation at platelet-marked sites of vascular injury and endothelial translocation as physiologic regulators of monocyte conversion to "inflammatory DC" capable of potent T cell stimulation in vivo (*14*, *15*). Deciphering pathways for a more physiologically relevant induction of monocyte-to-DC conversion will invite radical adjustments to the central paradigm of DC immunity and informed development of more effective DC-based therapies.

A clue toward physiologic DC production may be gleaned from an existing clinical treatment, extracorporeal photochemotherapy (ECP) (*16*, *17*), which uses an ex vivo modality to induce monocyte-to-DC conversion. This cellular immunotherapy, currently in wide therapeutic use for cutaneous T cell lymphoma (CTCL), is understood to facilitate rapid DC generation from blood monocytes in the absence of exogenous cytokines, solely through interaction of monocytes with peripheral blood components, including plasma proteins and activated platelets. The exact roles and mechanistic contributions of these blood constituents, often implicated in injury and inflammation, clotting, leukocyte extravasation, and wound healing, remain unresolved in literature. Recent studies of experimental ECP in murine models confirmed in vivo efficacy against melanoma, colon carcinoma (*16*), and ovarian cancer, although through unelucidated mechanisms of DC differentiation from blood monocytes (*18*). However, these studies identified platelets as a requisite constituent for therapeutic success.

Platelets are essential mediators of vascular homeostasis (*19*), hemostasis and thrombosis (*20*), and more recently, immunoregulation (*21*, *22*). Although activated platelets and platelet-borne molecules (e.g., P-selectin, CD40, secreted granules, etc.) have been shown to

[1]Department of Chemical and Environmental Engineering, School of Engineering and Applied Science, Yale University, New Haven, CT 06511, USA. [2]Department of Dermatology, School of Medicine, Yale University, New Haven, CT 06511, USA. [3]Department of Immunobiology, School of Medicine, Yale University, New Haven, CT 06511, USA. [4]Department of Biomedical Engineering, School of Engineering and Applied Science, Yale University, New Haven, CT 06511, USA. [5]Yale Flow Cytometry Facility, School of Medicine, Yale University, New Haven, CT 06511, USA. [6]Yale CINEMA Lab, School of Medicine, Yale University, New Haven, CT 06511, USA.
*These authors contributed equally to this work.
†Corresponding author. Email: tarek.fahmy@yale.edu (T.F.); redelson@yale.edu (R.E.)

direct leukocyte migration (*15*, *23*) and inflammatory stimulation (*24*), especially during infection or injury, the precise platelet-driven effects on monocyte function, particularly with regard to antigen processing and presentation, remain unexplored. Given accruing evidence of immunologically relevant cross-talk between platelets and monocytes (*19*), we investigated the role of platelets in initiating physiologic induction of DC. Here, we report that platelet-monocyte interaction, driven principally by engagement of platelet P-selectin with monocyte P-selectin glycoprotein ligand (PSGL1), culminates in the formation of a synaptic junction that directs the transformation of monocytes into cross-presenting APCs. Since this is a physiological strategy for DC production, we hence refer to these platelet-matured cells as physiological DC (phDC).

RESULTS

Peripheral blood mononuclear cells stimulate antigen-specific T cell responses in platelet-dependent manner

The impact of platelets on promoting peripheral blood mononuclear cell (PBMC)–mediated antigen-specific T cell stimulation was investigated as depicted in Fig. 1A. Platelet-containing ($PBMC^+pl^+$) or platelet-depleted ($PBMC^+pl^-$) PBMCs pulsed with endotoxin-free soluble ovalbumin (sOVA) model antigen were used to stimulate the clonal OVA–specific $CD8^+$ T cells derived from OT1 transgenic mice expressing T cell receptors (TCRs) specific for OVA peptide (SIINFEKL) presented within the context of major histocompatibility complex class I (MHC I). Platelets were routinely monitored in PBMCs collected from healthy mice (fig. S1A), and extent and specificity of platelet depletion were further confirmed by flow cytometry (fig. S1, C and D). PBMCs prepared with or without platelets were cultured overnight with sOVA, followed by a 3-day coculture with OT1 T cells (Fig. 1A).

Prominent differences in antigen-specific CD8 T cell responses were immediately observed between antigen-pulsed $PBMC^+pl^+$ and $PBMC^+pl^-$. Platelet-exposed PBMCs drove proliferative division of OT1 T cells, while platelet-depleted PBMCs demonstrated minimal proliferation (Fig. 1B). Titrated amounts of antigen pulsed to $PBMC^+pl^+$ and $PBMC^+pl^-$ confirmed the antigen specificity and platelet dependence of the T cell response (fig. S2A). A mock platelet depletion protocol using immunoglobulin isotype control was tested on $PBMC^+pl^+$ to demonstrate the T cell proliferation response as exclusively platelet dependent (fig. S2B).

Cytokine secretion and activation markers were also investigated. Consistent with robust proliferation, T cell incubation with $PBMC^+pl^+$ led to secretion of IL-2 and interferon-γ (IFNg) (Fig. 1C) at levels ~40-fold higher compared to naïve OT1 and generated antigen-experienced effector $CD25^+CD44^{hi}$ phenotypes (Fig. 1D), in stark contrast to $PBMC^+pl^-$. In the presence of platelets, activated T cells also expressed marginally increased levels of CD69, suggesting that these T cells are at later stages of activation (*25*), yet without loss of effector function as shown by production of granzyme B and lack of exhaustion marker PD1 expression (Fig. 1E and fig. S2C). T cell proliferation did not result in significant memory phenotype (fig. S2D). Despite reported immunomodulatory functions of platelet-expressed MHC I (*26*), isolated platelets pulsed with sOVA could not activate OT1 T cells, demonstrating insufficiency of platelets in direct priming of T cells and necessity for antigen processing and presentation mediated by PBMCs (fig. S2E). Together, these findings suggest that platelets specifically modify APCs in PBMCs to initiate robust antigen-dependent cytotoxic T lymphocyte (CTL) activation.

Monocytes in PBMCs are central to platelet-dependent T cell cross-priming

Given that PBMCs in the presence of platelets lead to robust T cell activation accompanied by expression of canonical cytokines and surface markers, we examined which components in the PBMCs are responsible for this platelet-dependent activation program. Although commonly associated with innate immunity and host defense, blood monocytes represent a sizable and readily available precursor population for generation of professional APCs in vitro and in vivo (*27*, *28*). We hypothesized that monocytes are both a necessary and sufficient PBMC subset for platelet-dependent immunogenic stimulation of T cells due to the following: (i) Antigen processing and presentation are required for antigen-specific T cell responses; (ii) circulating monocytes are capable of maturing into professional APCs, such as DCs; and (iii) platelets have been shown to aggregate with monocytes during inflammatory conditions (*15*, *23*).

To test monocyte involvement in T cell activation, we purified platelet-containing ($mono^+pl^+$) and platelet-depleted ($mono^+pl^-$) monocytes from PBMCs by negative selection (fig. S3A). Taking into consideration that monocytes make up to <10% of PBMCs, we found that $mono^+pl^+$ fully retained the T cell proliferation–stimulating function of $PBMC^+pl^+$, whereas $mono^+pl^-$ were as ineffective as $PBMC^+pl^-$ (Fig. 2A and fig. S3B). $mono^+pl^+$ and $mono^+pl^-$ obtained by fluorescence-activated cell sorting (FACS) further confirmed the monocyte requirement of the observed platelet-dependent effect (fig. S3, C and D). Consistent with previous results with unfractionated PBMCs, activation cytokines IL-2 and IFNg were significantly up-regulated exclusively during OT1 coculture with antigen-pulsed $mono^+pl^+$ (Fig. 2B). To further confirm T cell activation by monocytes, we checked the activation status of cocultured T cells and found similar induction of CTL phenotypes, CD25, CD44, and CD69 expression and granzyme B production, exclusively in platelet-exposed monocytes (fig. S4, A to C). In contrast, nonmonocytic portions of PBMCs failed to initiate immune activation regardless of platelet presence, establishing that the observed platelet-dependent effect is specific and limited to the monocyte subpopulation of PBMCs (fig. S4D). These observations are consistent with previous reports, indicating that monocytes can activate and proliferate T cells (*28*) yet, to our knowledge, represent the first example of platelet-driven activation of cross-presentation program in monocytes.

Maturation of immunogenic DCs is a direct effect of platelet-monocyte interactions

Cross-presentation is a mechanism by which exogenous antigen is processed and presented on MHC I, a characteristic requirement for the induction of antigen-specific effector $CD8^+$ T cell responses (*29*). Monocytes in circulation act as a precursor population to cell types such as myeloid-derived suppressor cells, macrophages, and DCs (*30*). While intrinsically able to take up, process, and present antigen, blood monocytes have been shown to primarily contribute to host defense and innate immunity, requiring additional phenotypic and functional differentiation to generate adaptive effector responses, especially through cross-presentation (*27*, *31*).

The observation that monocytes are principal participants in platelet-dependent activation of adaptive immunity prompted the search for a cross-presentation–competent population. We identified a $CD11b^+$ myeloid cell population exclusively present in platelet-exposed PBMCs up-regulating cross-presented sOVA peptide–loaded MHC I (SIINFEKL-H2Kb) (Fig. 2C). Consistent with characterizations

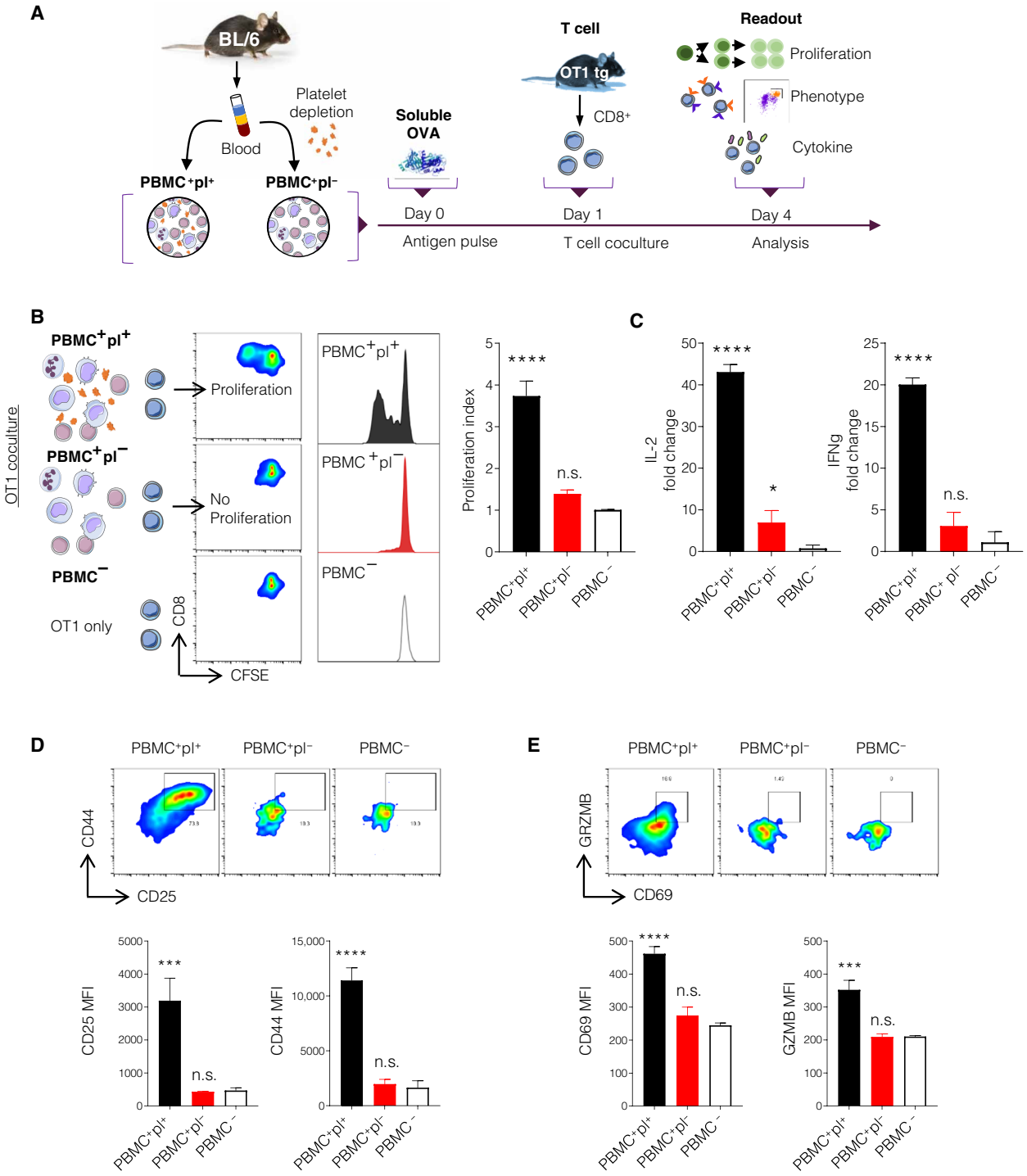

Fig. 1. Platelets are required for PBMC-driven antigen-specific CD8 T cell response. (**A**) Schematic of mouse experimental setup. Platelet-containing ($PBMC^+pl^+$) and platelet-depleted ($PBMC^+pl^-$) PBMCs were prepared from C57BL/6 mice. PBMC groups were incubated with endotoxin-free sOVA antigen overnight, followed by washing and 3-day coculture with carboxyfluorescein diacetate succinimidyl ester (CFSE)–stained OT1 T cells. T cells and supernatants were analyzed for proliferation, phenotype, and cytokines at end of coculture (day 4). tg, transgenic. (**B**) Fluorescence-activated cell sorting (FACS) analysis of naïve OT1 T cell proliferation induced by sOVA-pulsed $PBMC^+pl^+$ or $PBMC^+pl^-$ cultures, compared to OT1 alone ($PBMC^-$). Shown are (left) representative CFSE dilution FACS plots and histograms and (right) proliferation index of dividing OT1 T cells. (**C**) Enzyme-linked immunosorbent assay (ELISA) coculture supernatant quantifications for IL-2 (left) and IFNg (right). (**D** and **E**) Representative expression of (D) $CD25^+$, $CD44^+$, (E) $CD69^+$, and granzyme B (GRZMB) in cocultured OT1 T cells. All values are means ± SD of at least five independent experiments. One-way analysis of variance (ANOVA), $^{****}P < 0.0001$, $^{***}P < 0.001$, $^{*}P < 0.05$. n.s., not significant; MFI, mean fluorescence intensity.

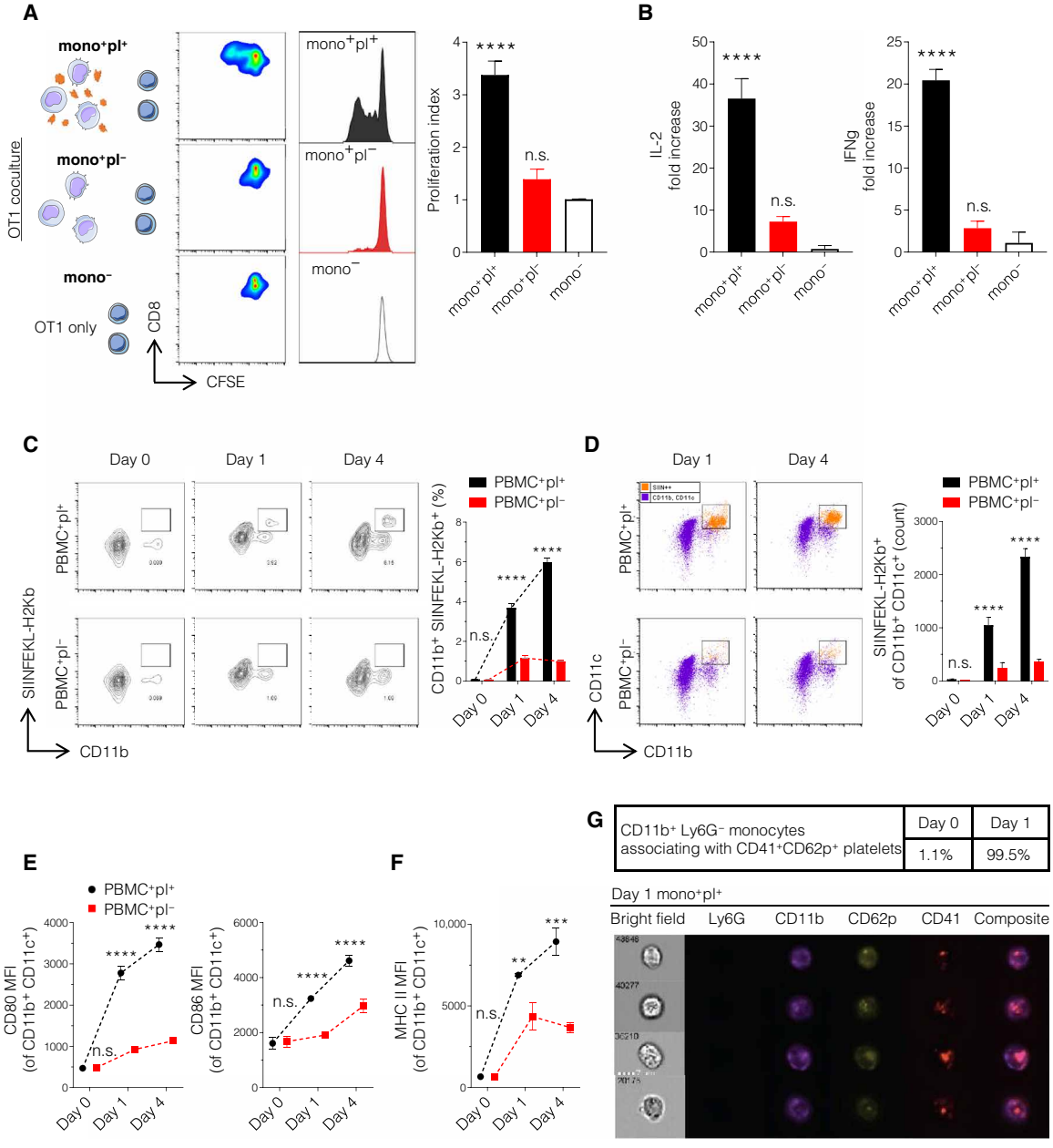

Fig. 2. Platelets interact with peripheral blood monocytes to activate antigen cross-presentation. (**A** and **B**) Platelet-containing (mono$^+$pl$^+$) and platelet-depleted (mono$^+$pl$^-$) monocytes purified from mouse PBMCs were incubated overnight with sOVA, followed by 3-day coculture with CFSE-stained OT1 T cells. (A) Flow cytometry analysis of mono$^+$pl$^+$, mono$^+$pl$^-$, and OT1 only (mono$^-$) cultures in triggering OT1 proliferation. Shown are (left) representative CFSE dilution FACS plots and histogram and (right) quantified proliferation index of dividing OT1 cells. (B) ELISA coculture supernatant quantifications for (left) IL-2 and (right) IFNg. (**C** to **F**) Flow cytometry analysis of DC surface marker evolution in PBMCs. Representative FACS plots of (C) (left) CD11b$^+$ cells expressing MHC I–loaded sOVA antigen, SIINFEKL-H2Kb, and (right) quantification (D) (left) SIINFEKL-H2Kb$^+$ CD11b$^+$ cells (orange) overlayed on CD11b and CD11c gated PBMCs (purple), and (right) quantification. (E and F) MFI of (E) (left) CD80 and (right) CD86 expression and (F) MHC II expression on CD11b$^+$ CD11c$^+$ cells in PBMC$^+$pl$^+$ (black) and PBMC$^+$pl$^-$ (red). (**G**) Representative Amnis images of CD11b$^+$ (purple) Ly6G$^-$ (blue) monocytes interacting with CD62p-expressing (yellow), CD41$^+$ (red) platelets, quantitated at days 0 and 1 in table above. All values are means ± SD of at least three independent experiments. (A and B) One-way ANOVA and (C to F) two-way ANOVA, ****$P < 0.0001$, ***$P < 0.001$, **$P < 0.01$.

of monocyte-derived DCs (*32*), we found that platelet presence in PBMCs (PBMC$^+$pl$^+$) yielded emergence of CD11c$^+$ subset of CD11b$^+$ population enriched with high levels of cross-presented antigen. In contrast, negligible generation of a CD11c$^+$ population or expression of SIINFEKL-H2Kb was observed from platelet-deficient PBMCs (PBMC$^+$pl$^-$) (Fig. 2D). Although cross-presentation has been demonstrated in monocyte-derived cells, particularly monocyte DCs (*28*), platelet association has not been implicated to influence antigen-presentation function. CD80 and CD86, two costimulatory markers indicative of APC maturation, were up-regulated only in presence of platelets, although CD83 did not show significant induction (Fig. 2E and fig. S4E). The increase in monocyte

MHC I–associated antigen, in combination with acquisition of cDC markers, suggests that monocytes are driven toward functional and phenotypic maturation into professional APCs via interaction with platelet components.

Conventional cultivation of bone marrow–derived DCs (BMDCs) requires differentiation cytokines IL-4/GM-CSF, followed by lipopolysaccharide (LPS) stimulation for maturation (*1*). Cytokine-derived BMDCs were compared against platelet-activated PBMCs and monocytes for their capacity for OT1 stimulation. We found that both PBMCs and monocytes performed at comparable levels as immature BMDCs, although PBMCs and monocytes were differentiated solely by platelets in the absence of cytokines and in one-sixth of the time (fig. S5A). CD14, the LPS receptor implicated in innate immune activation and a characteristic monocyte marker (*33*), also showed increased expression on monocytes in the presence of platelets (fig. S4F). However, no up-regulation of CD16 was observed (fig. S4G), although this marker had previously been associated with platelet-associated leukocyte inflammation (*34*). In their progressive phenotypic maturation, these platelet-interacting cells continue to exhibit a limited number of features with monocytes while transitioning into DC-like APCs characterized by rapid acquisition of functional capacity to cross-present antigen and cross-prime T cells.

Platelets showcased a capacity to rapidly differentiate circulating blood monocytes into APCs capable of robust adaptive immune stimulation, specifically through activation of cross-presentation programming. Platelet association resulted in another phenomenon prototypic of DC maturation (*14*, *16*), as $CD11b^+CD11c^+$ monocytes were also observed to up-regulate MHC II expression (Fig. 2F), further supporting that platelets may supplant inflammatory signals or maturation cocktails in generating DC-like APCs. To investigate the extent of platelet influence on APC functions of monocytes, particularly on MHC II–based antigen presentation, we examined OVA antigen–specific stimulation using $CD4^+$ OT2 transgenic T cells. Unexpectedly, OT2 coculture assays revealed little platelet dependence in leveraging antigen-specific OT2 proliferation, demonstrating a slight enhancement of OT2 stimulation by platelet-depleted PBMCs (fig. S5, B and C). This discrepant impact of platelets on OT1 and OT2 responses indicates that platelet interaction preferentially biases monocyte antigen processing toward MHC I loading. Previous work has shown platelet involvement in inflammatory processes central to innate host defense by monocytes in vivo (*24*, *35*) as well as assisting in cytokine-driven DC maturation in vitro (*36*, *37*); however, demonstration of platelets as sole initiators of adaptive immune functions in monocytes, especially cross-presentation in conjunction with DC maturation in absence of exogenous stimuli, has no precedence. Together, parallels between features of platelet-matured monocytes and canonical hallmarks of DCs suggest that platelets mediate differentiation of blood monocytes by invoking physiologic programs linking innate and adaptive immunity (*38*). We will, thus, refer to these platelet-matured monocytes as phDC.

To further understand how platelets mediate monocyte maturation, we monitored the platelet-monocyte interactions formed during the initial culture of platelet-containing PBMCs. Platelets exert precisely controlled physiologic functions in vivo, from effecting whole-body "life and death" reactions in hemostasis and thrombosis (*20*, *39*, *40*) to forming cellular microaggregates during inflammation (*41*), primarily relying on contact-based physical interactions not only among platelets but also with leukocytes. We used Amnis imaging to observe cell-cell contact between platelets and monocytes and found that platelets adhered to virtually all monocytes after overnight culture, with platelet-expressed CD62p (P-selectin) colocalized at platelet-monocyte interfaces, suggesting a role for a physical axis of interaction in the functional maturation of monocytes (Fig. 2G).

Platelet-derived P-selectin initiates monocyte activation and cross-presentation

We further investigated monocyte-platelet junctions by confocal microscopy to identify the stimulatory signaling axis driving monocyte cross-presentation. Platelet-containing PBMCs cultured overnight showed $CD11b^+$ $Ly6G^-$ monocytes forming junctions with $CD41^+$ platelets (Fig. 3A), confirming interactions previously visualized by Amnis. Three-dimensional (3D) reconstruction of platelet-monocyte structures highlighted P-selectin molecules on the surface of activated platelets bridging contact at the platelet-monocyte interface (movie S1), likely binding to monocyte PSGL1 (*42*).

Activation of platelets leads to secretion and display of a myriad of granule-stored molecules (*43*, *44*), most prominently CD40 and CD40L, cytokines transforming growth factor–β, CCL2, and IL-1β (*45*), and adhesion molecule P-selectin (*46*). To understand the mechanism of platelet-initiated phDC induction, we performed a series of studies targeted at such molecules known to facilitate platelet-monocyte interactions. Blocking, neutralizing, or substituting platelet molecules, CD40, CD40L, monocyte chemoattractant protein-1 (MCP-1), and dickkopf-1 (DKK-1), had little impact on monocyte cross-presentation (fig. S6, A and B). Confocal images further suggest that monocytes may be interacting with aggregates of platelets, prompting us to test blocking such aggregate formation using antibodies against CD41 or CD61 (fig. S6C). Although we did not observe any impact of blocking portions of $\alpha_{IIb}\beta_3$ on platelet surface, treating platelet-containing PBMCs with adenosine 5′-diphosphate receptor P2Y12 antagonist (*47*), Ticagrelor, abrogated subsequent T cell responses, implicating platelet activation in platelet-dependent monocyte cross-presentation (fig. S6D).

P-selectin is a platelet activation marker and an important modulator of platelet-leukocyte interactions, including adhesion, immobilization, and cell recruitment during tissue repair and thrombotic disorders (*41*, *46*); however, its significance in activating antigen cross-presentation machinery in monocytes is unknown. Therefore, we first investigated whether P-selectin contributes to observed platelet-dependent effects by testing whether recombinant P-selectin (P-selectin) recapitulates activation of antigen cross-presentation in PBMCs in the absence of platelets. Exposing sOVA-pulsed platelet-depleted PBMCs to culture dishes precoated with P-selectin restored cross-presentation, as demonstrated by the titratable recovery of antigen-dependent proliferation, activation-associated cytokine production, and OT1 T cell activation phenotypes (Fig. 3, B and C, and fig. S7A). We additionally tested the remaining two members of the selectin family and, unexpectedly, saw that E-selectin, but not L-selectin, also rescued platelet-depleted monocytes for cross-presentation (fig. S7B). As expected, neither P- nor E-selectin directly initiated T cell proliferation (fig. S7C), confirming that selectins specifically potentiated monocyte antigen cross-presentation, not nonspecific stimulation of T cells.

Both P- and E-selectin are cognate ligands for monocyte receptor, PSGL1 (*48*). PSGL1 initiates adhesion, rolling, recruitment, and extravasation of leukocytes, as shown in flow systems and in vivo (*49*, *50*), but its role in monocyte activation and differentiation is unexplored. We used an agonist anti-PSGL1 antibody (fig. S8, A and B) to investigate whether engaging this P-selectin receptor can trigger

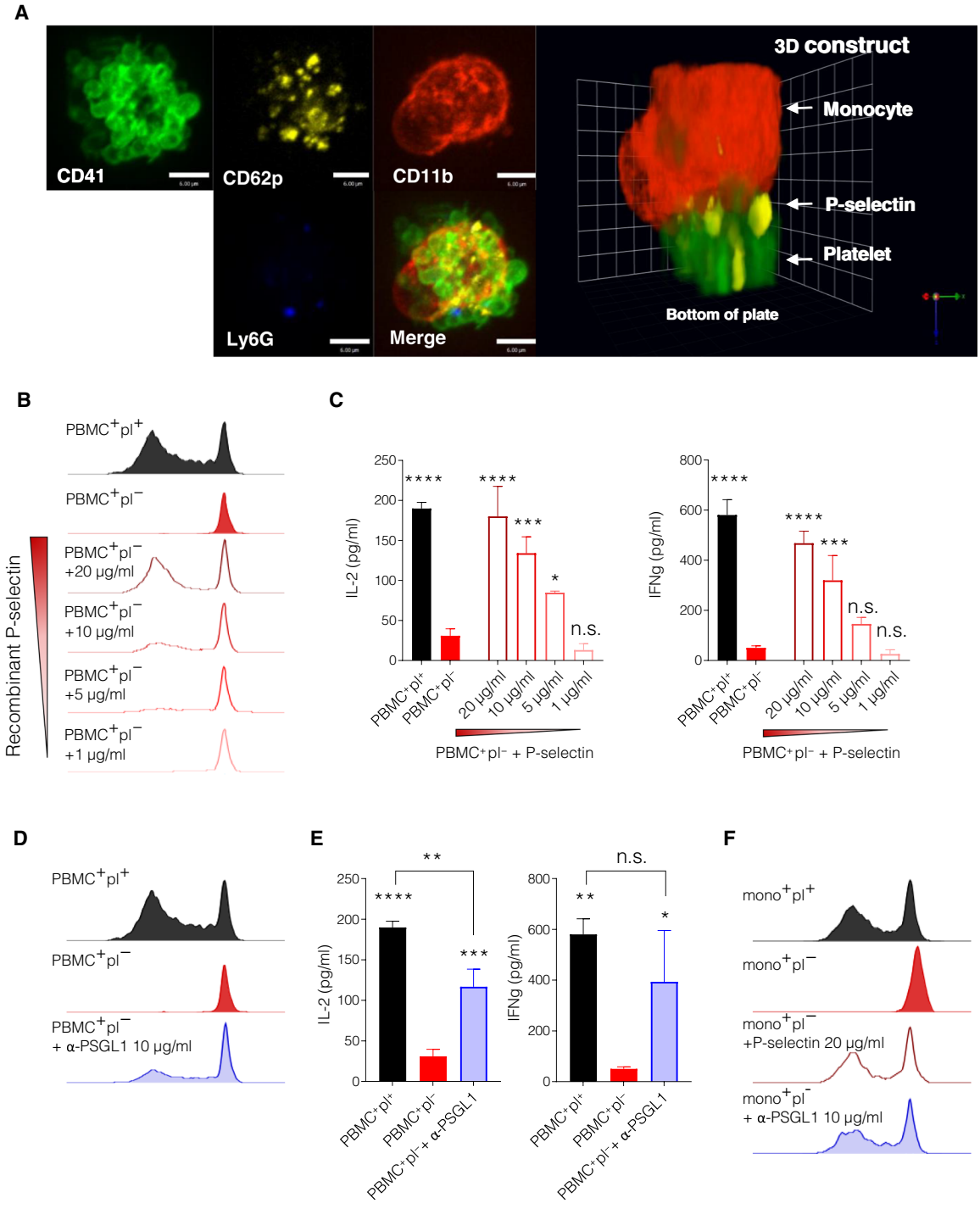

Fig. 3. P-selectin on platelets triggers enhanced cross-presentation via monocyte PSGL-1. (**A**) Live cell confocal microscopy of platelets interacting with monocytes in overnight cultures of murine PBMC$^+$pl$^+$. Top: CD41$^+$ (green) platelets expressing punctate CD62p (yellow) in association with CD11b$^+$ (red) Ly6G$^-$ (blue) monocyte. Bottom: 3D reconstruction highlights CD62p at platelet-monocyte interface. Scale bars, 6 μm. (**B** to **E**) OT1 T cell stimulation capacity of sOVA-pulsed PBMC$^+$pl$^+$ or PBMC$^+$pl$^-$ cultures treated with (B and C) varying concentrations of recombinant P-selectin (P-selectin) or (D and E) agonist anti-PSGL1 monoclonal antibody (mAb) (α-PSGL1). (B and D) Representative proliferation histograms of CFSE-stained OT1 T cells. (C and E) ELISA of (left) IL-2 and (right) IFNg. (**F**) Antigen-specific T cell stimulation capacity of sOVA-pulsed purified mono$^+$pl$^+$ or mono$^+$pl$^-$ cultures treated with P-selectin or α-PSGL1. Representative proliferation histograms of CFSE-stained OT1 T cells are shown. All values are means ± SD of at least five independent experiments. One-way ANOVA, $^{****}P < 0.0001$, $^{***}P < 0.001$, $^{**}P < 0.01$, $^{*}P < 0.05$.

monocyte cross-presentation. Treating platelet-depleted PBMCs with anti-PSGL1 leads to recovery of PBMC cross-presentation capacity for T cell activation in an agonist concentration–dependent manner, and anti-PSGL1 addition to platelet-containing PBMCs had no antagonist behavior (Fig. 3D and fig. S8C). Furthermore, anti-PSGL1–treated platelet-depleted PBMCs were shown to stimulate cytokine

production and cytotoxic phenotype generation consistent with T cells activated by platelet-containing PBMCs (Fig. 3E and fig. S8D). Purified monocytes yielded equivalent results to PBMCs when treated with P-selectin and anti-PSGL1, confirming specificity of P-selectin/PSGL1-dependent effects to monocytes within PBMCs (Fig. 3F and fig. S8E). These findings not only establish the P-selectin/PSGL1 axis as primary constituents in activation of cross-presentation in peripheral blood monocytes but also confirm platelets as the principal physiological driver for activation and maturation of monocytes to phDC.

P-selectin/PSGL1 interaction drives monocyte maturation and function in human PBMCs

Having demonstrated the role of P-selectin and its receptor PSGL1 in activating cross-presentation in murine peripheral blood monocytes, we extended our studies to human donor samples to determine whether this platelet-dependent functional maturation also occurs in human monocytes. Confocal imaging of monocytes purified from donor PBMCs and cultured overnight in the absence of platelets showed uniform surface expression of CD14 and PSGL1 (fig. S9A and movie S6). In platelet-containing culture, we immediately noticed that $CD61^+$ platelets induced monocyte PSGL1 to specifically cluster around platelet P-selectin–containing contacts to form "adhesion synapses" and even interactive platelet "bridges" between multiple platelets and monocytes (Fig. 4A and movie S2), reminiscent of the immunological synapse between APCs and lymphocytes. Formation of platelet-monocyte junctional complexes, accompanied by polarized PSGL1 localization, occurred exclusively in contact with activated platelets strongly expressing CD62p and displaying filopodial and lamellipodial extensions, while contact with resting $CD62p^-$ platelets did not bias PSGL1 distribution on monocytes (fig. S9, B and C, and movies S7 and S8). Cross-section analysis of the adhesion synapse further revealed that PSGL1 clustering surrounds multiple discrete nodes of P-selectin extending from platelets in a geometry reminiscent of a multipronged plug-and-socket connection (fig. S9D and movie S9). Despite polarization of PSGL1 in adhesion synapse formation with platelets, monocyte CD14 distribution remained constant in all cases, isolating platelet-monocyte interactions to P-selectin/PSGL1-mediated cell-cell contact.

We next designed an ex vivo system to investigate whether platelets can activate human blood monocytes to initiate antigen-specific T cell responses using clinically relevant tumor-associated antigens (TAAs) in combination with human TCR transgenic $CD8^+$ T cell lines. First, we tested platelet-containing and platelet-depleted human leukocyte antigen (HLA)–A2 donor PBMCs (fig. S1B) and their ability to present melanoma-associated antigen recognized by T cells long peptide (MART1 LP) to patient tumor-infiltrating lymphocyte (TIL)–derived MART1-specific DMF5 T cells (Fig. 4B) (*51*). Platelet-containing PBMCs yielded up to 10-fold enhancement over platelet-depleted PBMCs in inducing DMF5 T cell human IFNγ (hIFNg) production, as demonstrated with MART-1 antigen titrations (Fig. 4C). Recombinant human P-selectin was able to significantly restore the ability of platelet-depleted PBMCs to stimulate DMF5 (Fig. 4D, left), confirming that platelet P-selectin mediates enhanced antigen cross-presentation in human samples. To rule out the contribution of nonmonocytic PBMC compartments, we repeated the experiment with purified human monocytes (Fig. 4D, right). P-selectin–treated platelet-depleted monocytes showed no significant difference against platelet-containing monocytes in ability to cross-present antigen to DMF5.

We extended our studies to the human papilloma virus-16 (HPV-16) E7 oncoprotein, using E7-specific human T cells created by transgenic modification of human donor T cells (*52*). Our results with E7 LP align with findings for tumor antigen MART-1, similarly demonstrating absence of antigen presentation capabilities with platelet depletion and confirming that immunogenic antigen cross-presentation in human peripheral blood can be driven by platelets for several cancer-relevant antigens (Fig. 4E).

Continuing parallels between murine and human monocytes in platelet-dependent activation prompted us to check phenotypic maturation. Over 4 days of culture, $CD11c^+$ human monocytes in platelet-containing PBMCs significantly up-regulated expressions of CD86, HLA-DR, and HLA-A,B,C in comparison to monocytes in platelet-depleted culture (Fig. 4F). These data demonstrate that platelet-induced functional changes in antigen processing and presentation are accompanied by evolution of traditional DC phenotypes in human peripheral blood monocytes. Consistent with murine data, platelet presence up-regulated CD14 in human phDC. $CD14^+$ monocytes have been shown to differentiate into DC populations upon migration through inflamed endothelium (*14*, *32*), and CD14 is also known to initiate and regulate activation and DC life cycles through Src family kinase and Ca^{++}/calcineurin-dependent pathways in DC (*53*), strengthening the link between platelet-mediated monocyte maturation and physiological mechanisms of DC generation in vivo. Overall, evidence of P-selectin/PSGL1 signaling between platelets and monocytes, phenotypic monocyte maturation, and acquisition of functional cross-presentation capacity indicate platelet-dependent mechanisms of monocyte-to-DC differentiation in both murine and human assays.

Platelet-mediated signaling activates antigen processing and presentation pathways

P-selectin has been shown to induce leukocyte activation of Src and Src family kinases (*54*–*56*), mitogen-activated protein (MAP) kinase signaling (*57*), nuclear translocation of nuclear factor κB (NFκB) (*58*), and cytokine secretion (*59*), although prior reports have primarily focused on neutrophils (*55*–*57*). These signaling events, however, have proven essential for cytokine-mediated differentiation of DC from monocytes (*53*, *60*); thus, we assessed the activation of these pathways in platelet-exposed and platelet-deprived monocyte populations to identify platelet-initiated signaling pathways invoked in monocytes. Western blot analysis showed that platelet exposure leads to activation of Src kinase in monocytes, as indicated by an increase in Src phosphorylation (Fig. 5A). Src kinase is known to phosphorylate p85, the regulatory subunit of phosphatidylinositol 3 (PI3) kinase complex, resulting in integrin activation (*55*). The PI3 kinase signaling cascade also results in the phosphorylation and activation of Akt (*60*), which we also observe in platelet stimulated monocytes (Fig. 5A).

The Tec family kinase, Bruton tyrosine kinase (BTK), is activated via signaling events mediated by PI3 kinase (*61*) and the action of Src family kinases (*62*) and is implicated in the downstream signaling of PSGL1 (*56*). BTK, in turn, activates the MAP kinase pathway and phospholipase C–γ, which leads to calcium flux (*57*, *59*). Western blot analysis indicated that phosphorylated extracellular signal–regulated kinase (ERK) levels were elevated when monocytes were incubated with platelets (Fig. 5A), verifying the activation of the MAP kinase signaling axis. This led us to directly quantify calcium flux in platelet-exposed or platelet-depleted monocytes using calcium-specific

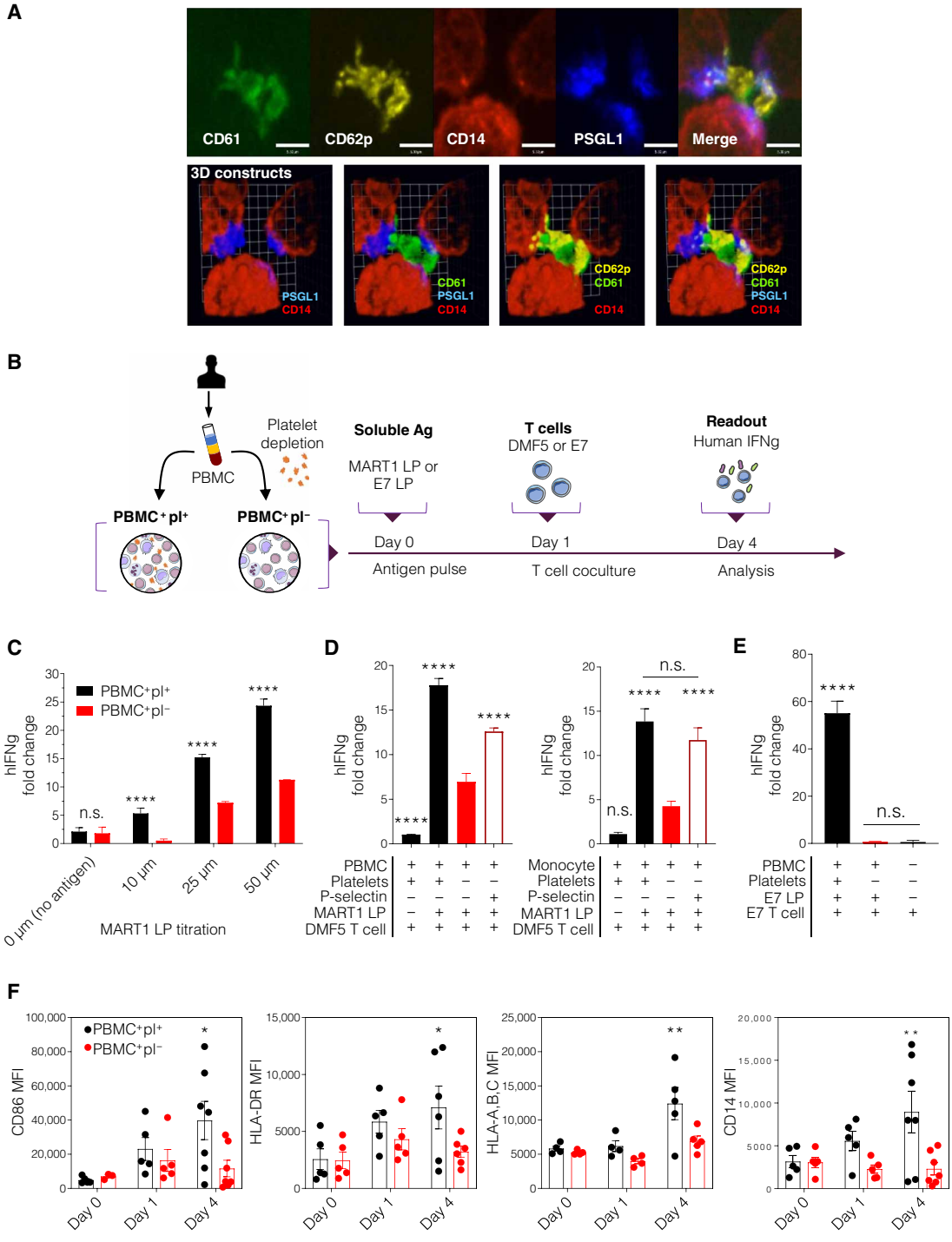

Fig. 4. Monocyte-platelet adhesion synapse formation drives antigen-specific immunity. (**A**) Top: Confocal imaging of purified human monocytes cultured with platelets overnight. Activated CD61$^+$ (green) platelets are shown forming CD62p$^+$ (yellow) and PSGL1$^+$-mediated junctions (blue) with CD14$^+$ (red) monocytes. Bottom: 3D reconstruction demonstrates punctate monocyte PSGL1 clustering around platelet CD62p. Scale bars, 5.30 μm. (**B**) Schematic of human experimental setup with soluble antigen (Ag). Platelet-containing (PBMC$^+$pl$^+$) and platelet-depleted (PBMC$^+$pl$^-$) PBMCs were prepared from healthy human donors. PBMC groups were incubated overnight with soluble tumor antigens, melanoma-associated antigen recognized by T cells long peptide (MART1 LP) or E7 LP, followed by washing and 3-day coculture with antigen-specific transgenic human T cells, DMF5 or E7, respectively. Supernatants were analyzed at end of culture (day 4). (**C** to **E**) Human IFNg (hIFNg) ELISA of (C) DMF5 cultured with PBMC$^+$pl$^+$ or PBMC$^+$pl$^-$ pulsed with MART1 LP at varying concentrations, (D) DMF5 cultured with MART1 LP–pulsed PBMC (left) or monocytes (right) with or without platelets or recombinant human P-selectin stimulation, and (E) E7 T cells cultured with E7 LP–pulsed PBMC$^+$pl$^+$ or PBMC$^+$pl$^-$ or E7 T cells only (PBMC$^-$). (**F**) FACS quantitation of CD86, HLA-DR, HLA-A,B,C, and CD14 in donor PBMCs at throughout incubation ($n = 5$ to 7). All values are means ± SD of at least three independent experiments. (C to E) One-way ANOVA and (F) two-way ANOVA, ****$P < 0.0001$, **$P < 0.01$, *$P < 0.05$. (F) Each point represents data from an individual healthy blood donor.

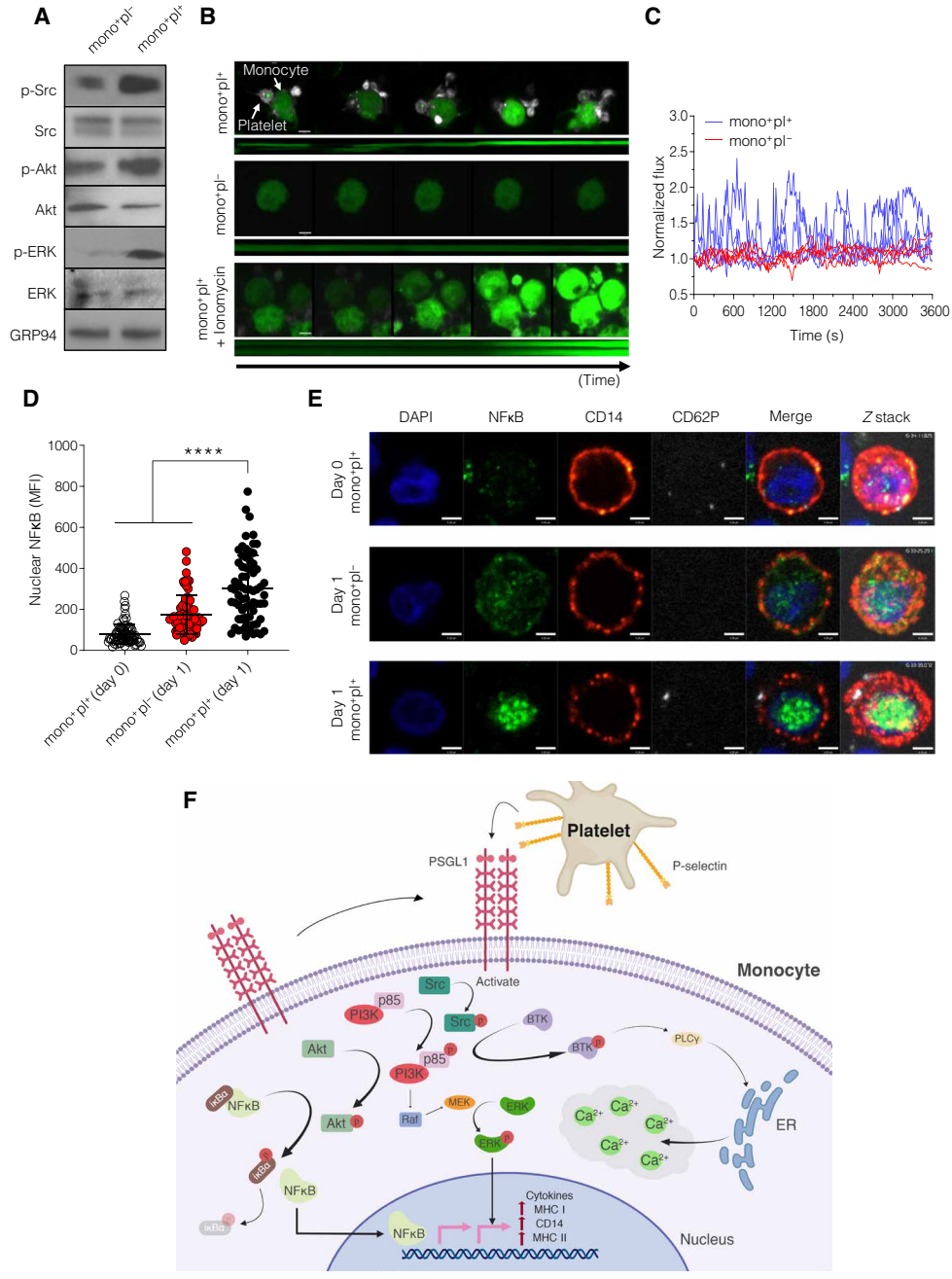

Fig. 5. Platelet-initiated monocyte signaling and activation pathways. (**A**) Purified monocytes from donor PBMCs were incubated with platelets (mono$^+$pl$^+$) or without platelets (mono$^+$pl$^-$) for 4 hours. Western blotting was carried out to assess phosphorylation status of Src, Akt, and extracellular signal–regulated kinase (ERK). GRP94 was used as a control to ensure equal protein in each lane. Data are representative of at least two biological replicates. (**B**) Confocal images (top of rows) and corresponding kymographs (bottom of rows) show calcium fluxing as observed by Fluo-4 (green) fluorescence intensity in freshly isolated monocytes with or without platelets (white). Ionomycin-activated monocytes are shown as positive control. Scale bars, 4.6 μm. mono$^+$pl$^+$, $n = 80$; mono$^+$pl$^-$, $n = 25$; mono$^+$pl$^+$ + ionomycin, $n = 30$. (**C**) Quantitation of calcium flux in representative mono$^+$pl$^+$ (blue) or mono$^+$pl$^-$ (red) monitored at 12-s intervals over 1 hour of imaging. (**D**) Nuclear translocation of NFκB quantified as MFI within 4′,6-diamidino-2-phenylindole (DAPI)–stained nuclei and (**E**) representative confocal images of mono$^+$pl$^+$ and mono$^+$pl$^-$ samples before (day 0) and after (day 1) overnight cultures stained with DAPI (blue), NFκB (green), CD14 (red), and CD62p (white) ($n = 67$ to 77 per group). Scale bars, 4.20 μm. (**F**) Illustration of demonstrated signaling pathways involved in platelet-dependent activation of cross-presentation in monocytes. Engagement of PSGL1 on monocytes by P-selectin on platelets initiates Src signaling that is known to activate PI3 kinase (PI3K), which, in turn, activates Akt that leads to the nuclear localization of NFκB. This leads to the up-regulation of MHC I and MHC II and the expression of cytokines. Src and PI3 kinase signaling is known to activate Bruton tyrosine kinase (BTK), which mediates calcium flux, activates MAP kinase pathway, and leads to the activation of transcription factors including NFκB. In the nucleus, NFκB and other activated transcription factors regulate the expression of cytokines, antigen processing and presentation machinery, and other costimulatory molecules. Molecules colored in green (Src, Akt, NFκB, ERK, and Ca2$^+$) were validated by our analyses. PLCγ, phospholipase C–γ; IκBα, inhibitor of NFκBα. All values are means ± SD of at least three independent experiments. One-way ANOVA, ****$P < 0.0001$.

dye Fluo-4. As shown by both confocal imaging and corresponding kymographs, platelet-exposed monocytes show significantly increased calcium-associated signal (Fig. 5B, top, and movie S3) compared to platelet-depleted monocytes (Fig. 5B, middle, and movie S4) at levels comparable to ionomycin stimulation (Fig. 5B, bottom, and movie S5). Together with Src, ERK, and Akt signaling, continuing cycles of calcium-fluxing platelet-exposed monocytes as quantitated (Fig. 5C) confirm platelet-associated activation of signaling pathways also reported to be essential in monocyte-to-DC differentiation (*60*).

The Akt, BTK, and ERK signaling pathways are also upstream regulators of NFκB signaling, a major immune cell pathway controlling transcription, cytokine production, and cell survival (*58*, *60*, *63*). Platelet-initiated NFκB nuclear translocation was verified by confocal imaging of platelet-exposed or platelet-depleted PBMC-borne monocytes (Fig. 5, D and E). ERK and NFκB signaling pathways are known regulators of DC antigen processing and presentation machinery (*63*, *64*), costimulatory molecule expression, and cytokine secretion (*59*, *65*). As summarized diagrammatically in Fig. 5F, our results showing platelet-driven activation of several signaling pathways in monocytes establish demonstrable links between signaling through the P-selectin/PSGL1 axis and increases in antigen cross-presentation observed in phDC.

Evidence for platelet-matured DCs initiating anticancer immunity

While soluble antigens make important experimental tools, dying tumor cells are an antigen source with direct clinical relevance to cancer immunology. Mounting an effective adaptive immune response in vivo requires APCs to overcome hurdles in internalizing, processing, and cross-presenting complex cellular antigens. To examine whether phDC could generate anticancer immunity using complex antigen sources, we challenged our platelet-matured mouse and human phDC with apoptotic tumor cells for stimulation assays with tumor antigen–specific T cells. A clinically used ultraviolet A (UVA)–photoactivatable chemotherapy agent, 8-methoxysoralen (8-MOP), was used to induce controlled immunogenic tumor cell death (*66*, *67*).

Platelet-containing or platelet-depleted mouse PBMCs were cocultured overnight with OVA-expressing melanoma, B16OVA, which was treated with 8-MOP/UVA in dosage sufficient to induce immunogenic cell death (*67*) to allow for tumor antigen acquisition (Fig. 6A). Only platelet-exposed PBMCs were able to cross-present tumor cell–derived antigen to induce antigen-specific OT1 $CD8^+$ T cell proliferation (Fig. 6B) and stimulate inflammatory cytokine production (Fig. 6C). Apoptotic B16OVA tumor cells alone were unable to stimulate an antigen-specific response, suggesting APC costimulation requirement by naïve OT1 T cells; platelet-depleted PBMCs also failed to induce T cell stimulation, paralleling observations from using sOVA. Unexpectedly, B16OVA-loaded BMDCs were not able to generate a robust T cell proliferation to match that of platelet-containing PBMCs, possibly indicating superior capacity for platelet-matured phDC to process complex cellular antigens (fig. S10). Furthermore, cytotoxic effector:target ratio assays using differentially stimulated effector T cells with live B16OVA tumor targets revealed that OT1 T cells stimulated with platelet-containing PBMCs or monocytes show highest antitumor efficacy (Fig. 6D), significantly exceeding the cytotoxicity of OT1 stimulated by tumor-loaded BMDCs or controls.

With considerations for clinical tumor immunotherapy, we extended our analyses to human donor cells and TAA-expressing patient-derived tumor cells to test human tumor–loaded phDC in generating antigen-specific T cell responses. As outlined in Fig. 6A, PBMCs prepared from HLA-A2 donor blood in presence or absence of autologous platelets were cocultured with 8-MOP/UVA–treated tumor cells from two different malignancies, melanoma or head and neck squamous cell carcinoma. Capacity for cross-presentation was then evaluated using tumor antigen–specific human TCR transgenic T cells, DMF5, E6, and E7, for readouts.

We first used primary melanoma MART-$1^{(+)}$ (YUCOT) or MART-$1^{(-)}$ (YUSIV and YUSOC) tumor cell lines derived and sequenced by the Yale Dermatology Specialized Programs of Research Excellence (SPORE) Specimen Resource Core (*68*) to generate apoptotic tumor antigen sources (*67*) and platelet-exposed or platelet-depleted PBMCs as APCs. Significant DMF5 stimulation was observed in the presence of MART-1^+ YUCOT–loaded platelet-containing PBMCs, demonstrating the generation of cross-presenting antitumor human phDC solely from autologous platelets, PBMCs, and dying tumor cells (Fig. 6E).

The remarkable ability of platelets to cue cross-presentation prompted us to explore the role of platelets in skewing uptake and processing capabilities in phDC. We analyzed internalization and intracellular localization of PKH-labeled apoptotic YUCOT by Amnis imaging and found that platelet-exposed human phDC exhibited less than 25% difference in amount of phagocytosed tumor cells compared to platelet-depleted monocytes (Fig. 6F). Intracellular sequestration of antigen outside the traditional phagolysosome has been proposed as one explanation for the cross-presentation competence of DC (*69*). Thus, we quantitated tumor material either localizing in, or outside of, fluorescently labeled lysosomal compartments. Unexpectedly, extralysosomal localization of tumor antigen increased more than twofold in platelet-exposed phDC (Fig. 6, G and H), suggesting that platelet-interactions could be activating phDC for enhanced cross-presentation through mechanisms promoting extralysosomal localization of antigen.

To explore translational opportunities for personalized phDC-based immunotherapy, we examined the ability to generate autologous responses from donor-derived transgenic T cells. Extending our investigations beyond melanoma to an oropharyngeal cancer associated with HPV infection, we challenged donor phDC to cross-present viral tumor oncoprotein antigens using HPV-16 E6/E7-positive head and neck squamous cell carcinoma (HPV^+ SCC61) (*70*). T cells from an individual healthy blood donor were transduced with HPV E6 and E7 antigen–specific TCRs and stimulated with autologous PBMCs or monocytes loaded with 8-MOP/UVA–treated HPV^+ SCC61. Platelet-exposed PBMCs or monocytes elicited significantly enhanced hIFNg responses in autologous E6 (Fig. 6I) and E7 (Fig. 6J) T cells, while platelet-depleted PBMCs or monocytes presented no observable increase in cross-presentation capacity. This not only demonstrates the therapeutic generalizability of human phDC to treatment of antigenic malignancies beyond melanoma but also affirms the potential for personalized immunotherapy using patient-derived, platelet-matured phDCs and T cells.

Together, these results confirm that cross-presentation–competent human phDC can be induced specifically through activated platelet interaction with primary monocytes, creating potent therapeutic APCs with a variety of immunologically relevant antigen sources. These findings open the possibility of phDC clinical use in design of personalized cancer immunotherapies.

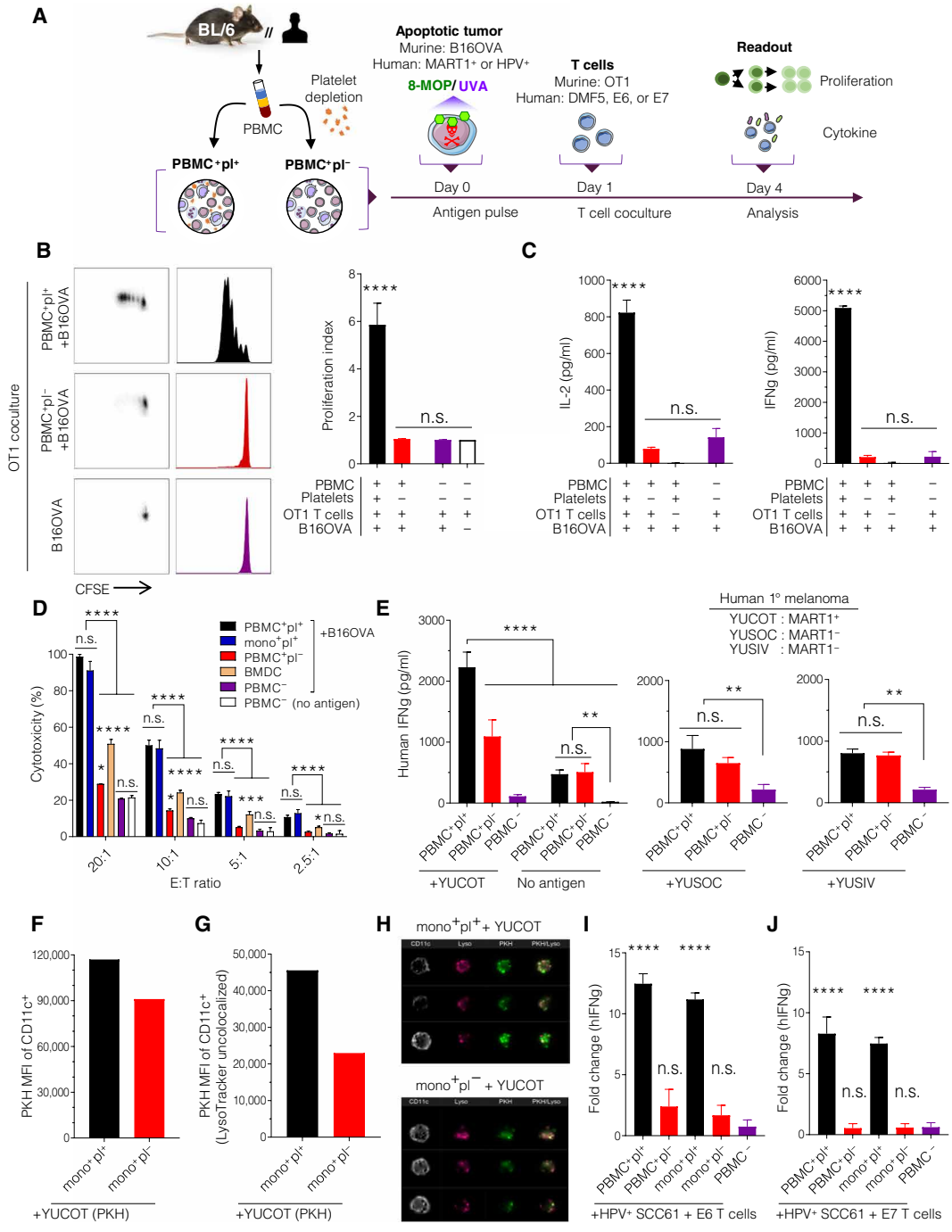

Fig. 6. Evidence for platelet-mediated DC maturation for cancer immunotherapy. (**A**) Schematic of experimental setup with apoptotic tumor cells as antigen. Platelet-containing ($PBMC^+pl^+$) and platelet-depleted ($PBMC^+pl^-$) PBMCs were prepared from C57BL/6 mice or healthy human donors. PBMC groups were incubated overnight with apoptotic murine B16OVA or human tumor cells rendered apoptotic by 8-MOP/UVA, followed by washing and 3-day coculture with OT1 T cells or antigen-specific transgenic human T cells, respectively. T cells and supernatants were analyzed at end of coculture (day 4). (**B**) FACS analysis of OT1 T cell proliferation triggered by apoptotic B16OVA-pulsed $PBMC^+pl^+$, $PBMC^+pl^-$, or OT1-only ($PBMC^-$) cultures. Shown are (left) representative CFSE dilution FACS plots and histograms and (right) proliferation index of dividing OT1 T cells. (**C**) Coculture supernatant ELISA for IL-2 (left) and IFNg (right). (**D**) Cytotoxic activity of OT1 T cells proliferated by apoptotic B16OVA-pulsed $PBMC^+pl^+$, $PBMC^+pl^-$, or bone marrow-derived DCs (BMDC), by apoptotic B16OVA alone ($PBMC^-$ + B16OVA), or without antigen ($PBMC^-$), against live B16OVA tumor cells at multiple effector:target (E:T) ratios. (**E**) hIFNg supernatant ELISA of DMF5 T cells cocultured with $PBMC^+pl^+$, $PBMC^+pl^-$, or DMF5 only ($PBMC^-$), with or without apoptotic $MART1^+$ YUCOT, $MART1^-$ YUSOC, or $MART1^-$ YUSIV melanoma. $mono^+pl^+$ or $mono^+pl^-$ cultures stained with LysoTracker (red) were incubated overnight with apoptotic YUCOT melanoma (PKH, green). (**F** to **H**) Amnis imaging analysis for (F) total uptake as reported by MFI of intracellular PKH within $CD11c^+$ monocytes, (G) extralysosomal tumor localization as reported by MFI of LysoTracker-uncolocalized intracellular PKH, and (H) representative images. (**I** and **J**) hIFNg supernatant ELISA of (I) HPV E6– or (J) HPV E7–specific human T cells cocultured with $PBMC^+pl^+$, $PBMC^+pl^-$, $mono^+pl^+$, $mono^+pl^-$, or T cells only ($PBMC^-$), with or without apoptotic HPV^+ SCC61 squamous cell carcinoma. All values are means ± SD of at least two independent experiments. One-way ANOVA, $^{****}P < 0.0001$, $^{***}P < 0.001$, $^{**}P < 0.01$, $^{*}P < 0.05$.

DISCUSSION

Our studies identify platelets and platelet-associated molecules as key inducers of monocyte maturation into cross-presenting cells resembling DC, referred to here as phDC due to their physiological, platelet-driven formation without use of exogenous cytokines. When pulsed with soluble or complex cellular tumor antigens, phDC induced from mouse or human blood monocytes exhibited remarkable capacity for stimulation of naïve, primary antigen-specific $CD8^+$ T cells, in stark contrast to monocytes cultured under platelet-deficient conditions. These suggest that physiological interactions with platelets initiate monocyte-to-DC maturation over a single day, in the absence of added cytokines. Our findings that a limited repertoire of progenitor monocyte features is maintained even after acquiring phenotypic and functional hallmarks characteristic to conventional DC suggest that after transition into phDC, the resulting APCs may undergo further maturation locally in physiologic sites of inflammation or insult that warrant encounters with activated platelets.

It is increasingly recognized that platelets deploy stores of preformed molecules such as junctional adhesion molecule C, GpIb (glycoprotein Ib), and, most prominently, CD40L (CD154) (*19*, *38*) during inflammation and promote leukocyte maturation. However, no previous reports have directly linked platelet interaction with activation of antigen cross-presentation capacity in monocytes. Here, we identify platelet P-selectin as the principal initiator of monocyte cross-presentation programming, a hallmark of adaptive immune control by professional APCs. Platelet P-selectin formed an adhesion synapse signaling axis by binding to monocyte PSGL1, triggering activation and DC-associated phenotypic changes. Although the geometries formed differ from the "bulls-eye" model of the supramolecular activation cluster (*71*), the monocyte-platelet adhesion junction demonstrates contact-dependent polarization of PSGL1 on monocyte surfaces and suggests dynamic molecular reorganization upon interaction with platelet P-selectin. We hypothesize that the activation synapse between platelets and monocytes acts not only as a tethering interface but also as a dynamic adaptive controller, liken to the immunological synapse between APCs and T cells, modulating P-selectin–mediated activation of PI3 kinase signaling, calcium fluxing, and NFκB translocation, as well as, functionally, cross-presentation and DC-maturation (*72*). Although we identified P-selectin as the primary initiator of platelet-dependent DC maturation and cross-presentation, our studies do not exclude a role for other platelet-borne molecules in linking platelets to adaptive immune functions of blood monocytes.

As part of maintaining tissue homeostasis and immunosurveillance, platelets act as bridges and "pathfinders" for recruiting blood monocyte into inflamed endothelium in vivo (*15*, *23*, *73*). Since tissue transmigration/transendothelial trafficking has previously been shown to signal monocyte differentiation for DC conversion (*14*, *74*), our finding that only platelet- and endothelial-associated P- and E-selectins, but not lymphocyte-associated L-selectin, confer cross-presentation capacity on monocytes that further supports intrinsic ties between inflammation in the vasculature, platelets, and monocyte maturation. However, activation of platelets that lead to up-regulation of P-selectin and hemostatic events does not occur spontaneously in vivo. Monocytes and platelets exist in extremely close proximity in the circulation and tissues, and the lack of unprompted or undesirable monocyte activation or thrombotic events indicates that these blood components remain in a tightly controlled, inactivated state under steady-state conditions until signaled by insults such as infection or inflammation (*45*, *46*). Our data indicate that our platelet/monocyte culture system may co-opt the in vivo conditions, normally leading to monocyte activation and DC differentiation during diapedesis, as has been previously suggested by studies using in vitro flow systems (*66*). This evidence, together with demonstrated platelet-dependent signaling cascades central to innate immune activation and adaptive immune function, leads us to speculate that rapid production of therapeutic phDCs from platelet-monocyte interactions leverages physiologic pathways in which platelets intimately connect innate immune processes of wound healing and inflammation to activation of adaptive immunity through in vivo DC differentiation.

Our finding that phDCs mount a robust antigen-specific CTL response against live tumor cells, outperforming cytokine-derived BMDCs, suggests that leveraging physiologic interactions in generating functional DC may be critical for in vivo immunotherapeutic applications. A renewed attention to platelets as a key regulator of physiologic functions and disorders may provide new immunologic insights into previously ill-understood phenomenology. In particular, platelet involvement may explain previous reports of spontaneous DC generation from cultures of whole PBMC preparations (*75*). Furthermore, our proposed production of cross-presentation–competent, activated platelet–induced phDC cements the mechanism of ECP as one driven by platelet-initiated monocyte-to-DC transition during flow-based ex vivo interactions of PBMCs (*76*), resolving a clinical enigma that has endured since ECP's introduction 30 years ago until its widespread use today. Our findings further corroborate results from experimental ECP as applied to murine in vivo solid tumor models (*16*), which exhibited complete loss of therapeutic efficacy upon platelet removal. This platelet-dependent in vivo relevance is strongly supported by data, confirming that DC differentiation was absolutely dependent on the presence of activated platelets in ECP model systems, where monocyte-to-DC maturation was completely blocked by monoclonal anti–P-selectin antibodies (*76*) and where DC-dependent successful antimelanoma effects in vivo were completely abrogated by the removal of platelets from the experimental ECP system (*16*). Implications of translation to future designs of DC-based immunotherapies for cancers beyond CTCL and, potentially, opportunistic infections are particularly notable, as our insights are drawn from an existing Food and Drug Administration–approved clinical therapy. To this end, our results in generating patient-specific T cell responses against HPV^+ tumor cells using patient-derived phDC represent a seminal step toward clinical implementation of platelet-driven DC maturation for directed personalized immunotherapy.

MATERIALS AND METHODS

Animals

C57Bl/6J and B6.SJL-*Ptprc*^{a} *Pepc*^{b}/BoyJ (B6.SJL CD45.1) mice were purchased from the Jackson Laboratory. OT1 CD45.2 [C57Bl/6-Tg (TcraTcrb)1100Mjb/J] mice that recognize OVA peptide residues 257 to 264 in the context of H2Kb were purchased from the Jackson Laboratory. OT2 CD45.2 [C57/Bl/6-Tg(TcraTcrb)425bn/J] mice that recognize OVA peptide residues 323 to 339 in the context of I-Ab were purchased from the Jackson Laboratory. Age- and sex-matched mice that were at least 9 weeks of age were used for all experiments. Experiments were performed according to the Yale Institutional

Animal Care and Use Committee–approved animal protocols, in agreement with the National Institutes of Animal Healthcare Guidelines. Mice were maintained under specific pathogen–free conditions, food, and water provided ad libitum. The animal facility is accredited by the Association for Assessment of Laboratory Animal Care.

Cell culture

RPMI 1640, Dulbecco's modified Eagle's medium (DMEM), OptiMEM, and media supplements were obtained from Invitrogen, Carlsbad, CA unless otherwise noted. Complete RPMI 1640 (cRPMI) media were made by supplementing RPMI 1640 with 10% heat-inactivated fetal bovine serum (FBS) (HyClone), 10 mM Hepes, 1% nonessential amino acids, 2 mM L-glutamine, 1 mM sodium pyruvate, 0.05 mM β-mercaptoethanol, and antibiotics. All cell lines were cultured at 37°C in 5% CO_2. B16F10 cells (provided by M. Bosenberg, Yale University, New Haven, CT) were grown in DMEM supplemented with 10% FBS and 1% penicillin/streptomycin. B16F10 melanoma cells expressing truncated cytoplasmic OVA (B16OVA, clone M05.F5, provided by L. D. Falo, Jr., University of Pittsburgh School of Medicine) were maintained in cRPMI with Geneticin G418 (1 mg/ml). YUCOT, YUSOC, and YUSIV human melanoma cell lines (received from the Yale SPORE Skin Cancer Core) were grown in OptiMEM media containing 5% FBS and 1% penicillin/streptomycin. HPV^- SCC61 and HPV^+ SCC61 (obtained from W. Yarbrough, Yale Department of Surgery) were cultured in DMEM/F12 with 10% FBS, hydrocortisone (0.4 μg/ml), and 1% penicillin/streptomycin. DMF5 [gift of J. R. Wunderlich, Surgery Branch Cell Prep Core, National Cancer Institute (NCI)], HPV E6 and HPV E7 (gift of C. Hinrichs, NCI Clinical Research Center) TCR transgenic T cell lines were cultured in AIM V media supplemented with 10% Lonza hAB serum and recombinant human IL-2 (600 IU/ml). All cell lines are routinely tested for *Mycoplasma* by standard polymerase chain reaction methods at each cell batch freezing. Cells were used for experiments within one passage of thawing a frozen aliquot.

Isolation of murine PBMCs

Peripheral blood was collected from mice via superficial temporal vein or retro-orbital plexus into containers containing 1:100 of heparin (5000 U/ml; McKesson Packaging Services) unless otherwise stated. To compare the effects of different anticoagulants on platelet activation, blood was collected in Vacutainers precoated with heparin as described above. Platelet-containing PBMCs were isolated from peripheral whole blood via Lympholyte M (Cedarlane Labs) gradient separation, followed by ACK buffer (Lonza) red blood cell lysis.

Platelet depletion from murine PBMCs

CD41 Biotin and subsequent Anti-Biotin MicroBeads with column magnetic separation (Miltenyi Biotec, 130-105-869, 130-090-485, and 130-042-401) were used for platelet depletion from murine PBMCs. Platelet depletion was confirmed by quantitation Hemavet hematology counter (Drew Scientific, HV950FS).

Monocyte isolation from murine PBMCs

Two micrograms each anti-mouse biotin cocktail composed of CD3ε (BioLegend #100304), LY6G (BioLegend #127604), NK1.1 (BioLegend #108704), CD45/B220 (BioLegend #103204), and CD19 (BioLegend #115504) and subsequent Anti-Biotin MicroBeads and column magnetic separation (Miltenyi Biotec, 130-090-485 and 130-042-401) were used for the negative selection of murine monocytes. Anti-mouse CD41 biotin and anti-mouse biotin monocyte cocktail (as described above) were combined with subsequent Anti-Biotin MicroBeads and column magnetic separation for the isolation of platelet-depleted monocytes from murine PBMCs. Monocyte isolation purity was confirmed by flow cytometry, while platelet content was monitored by Hemavet analysis.

BMDC generation

BMDCs were derived in vitro from femur and tibia bone marrow cells of C57/Bl/6J mice. Marrow was flushed from bones using a 25-gauge needle with cell culture media. After passing through a 40-μm cell strainer, red blood cells were lysed from bone marrow using ACK lysis buffer and plated in cell culture media containing GM-CSF (20 ng/ml). After 5 days, nonadherent cells were washed and replated in fresh GM-CSF–supplemented media and incubated for 48 hours more. Nonadherent cells were removed, washed, and used immediately for experiments with immature BMDCs. LPS-stimmed BMDCs were prepared by stimulating immature BMDCs with LPS (50 ng/ml) for 4 hours under standard culture conditions.

Incubation of murine PBMCs, BMDCs, or monocytes with soluble and cellular antigen

Platelet-containing or platelet-depleted murine PBMCs, monocytes, or BMDCs were cultured at 2.5×10^6 cells/ml overnight under standard conditions in RPMI 1640 without phenol red (Invitrogen, Carlsbad, CA) supplemented with 15% autologous mouse serum, 1% penicillin/streptomycin, and 1% L-glutamine. OVA was added at 50 μg/ml to PBMCs or monocytes during overnight culture. EndoFit (InvivoGen) OVA was used unless otherwise stated. For cultures with apoptotic tumors as cellular antigen, 1.25×10^6 tumor cells/ml were added for overnight culture. After overnight culture, cells were harvested, washed, and plated in 96-well plates in cRPMI.

PBMC and monocyte stimulation and inhibition

Tissue culture plates were coated with Fc-chimeric P-selectin (CD62P, BioLegend #755404), E-selectin (CD62E, BioLegend #755504), and L-selectin (CD62L, BioLegend #772806) for up to 3 hours under standard culture conditions before addition of cells for overnight culture at 20 μg/ml unless otherwise indicated. Tissue culture plates were coated with anti-mouse PSGL1 antibody (4RA10, BD Biosciences #557787) for up to 3 hours under standard culture conditions before addition of cells for overnight culture at 10 μg/ml, unless otherwise indicated. Blocking with anti-mouse CD40 (HM40-3, BioLegend #102908), CD40L (MR1, BioLegend #106508), MCP-1 (2H5, BioLegend #505905), CD41 (MWReg30, BioLegend #133910), or CD61 (2C9.G2, BioLegend #104310) and experiments with Ticagrelor (Sigma-Aldrich) and DKK-1 (BioLegend #759604) were performed by addition to PBMCs before overnight culture. Thrombin (Sigma-Aldrich) was added to the collected PBMCs for 30 min before analysis.

T cell labeling and isolation

Spleens from OT1 and OT2 transgenic mice (aged 10 to 14 weeks) were collected and dissociated into single-cell suspensions. Red blood cells from OT1 and OT2 splenocytes were lysed using ACK lysis buffer and labeled with carboxyfluorescein diacetate succinimidyl ester (CFSE) at 5 μM. Labeled cells were washed using 5× volume of cRPMI, and $CD8^+$ or $CD4^+$ T cells from OT1 or OT2 splenocytes

were isolated using negative selection kits STEMCELL EasySep Mouse CD8 (#19853) or CD4 (#19852) T cell isolation kit, respectively, according to the manufacturer's protocols.

T cell proliferation and cytokine secretion assays

CFSE-stained T cells were cocultured at 1×10^6/ml in 96-well plates with 1×10^6/ml of antigen-loaded PBMCs or 1×10^5/ml of antigen-loaded monocytes. Cells were cocultured in cRPMI for 3 days under standard conditions. At the end of coculture, cell proliferation indicated by CFSE dilution was assessed by flow cytometry (Attune NxT, FlowJo X). Coculture supernatants were collected and analyzed for IL-2 (BD #555148) and IFNg enzyme-linked immunosorbent assay (ELISA) (BD #555138) per the manufacturer's instructions.

Mouse flow cytometry analysis

Cells were stained following standard protocols. Experiments used antibodies specific for mouse Fc receptor (FcR) block (93, BioLegend #101320), CD8 (53-6.7, BioLegend #100712), CD45.2 (104, BioLegend #109830), CD44 (IM7, BioLegend #103032), CD69 (H1.2F3, BioLegend #104508), PD1 (29F.1A12, BioLegend #135214), KLRG1 (2F1/KLRG1, BioLegend #138408), CD11b (M1-70, BioLegend #101206), CD11c (N418, BioLegend #117320), SIINFEKL-H2Kb (25-D1.16, BioLegend #141608), CD80 (2D10, BioLegend #305232), CD83 (Michel-19, BioLegend #121510), CD86 (GL-1, BioLegend #105014), MHC II (M5/114.15.2, BioLegend #107624), granzyme B (QA16A02, BioLegend #372212), CD16 (93, BioLegend #101326), CD14 (M14-23, BioLegend #150106), Ly6G (1A8, BioLegend #127617), F4/80 (BM8, BioLegend #133914), CD115 (AFS98, BioLegend #135510), CD63 (NVG-2, BioLegend #143906), CD154 (MR1, BioLegend #106505), CD61 (2C9, BioLegend #104306), CD62p (RMP-1, BioLegend #109220), CD41 (MWReg30, BioLegend #133912), CD3 (17A2, BioLegend #100210), CD19 (6D5, BioLegend #115520), NK1.1 (PK136, BioLegend #108714), B220 (RA3-6B2, BioLegend #103240), CD25 (PC61, BD Pharmingen #553866), and CD127 (A7R34, eBioscience 45-127-80). Color-matched isotype control antibodies were obtained from the same vendors. Stratedigm or Attune NxT flow cytometer was used to gate set on live cells by 7-aminoactinomycin D (7-AAD) Viability Staining (BioLegend #420404), EMA (Invitrogen E1374), or Zombie NIR (BioLegend #423106) exclusion. A minimum of 3×10^4 events were collected per sample. Data were analyzed with FlowJo 10 software (FlowJo LLC).

T cell–mediated cytotoxicity

Lactate dehydrogenase (LDH) release assay (Roche, Penzberg, Germany) was used to measure OT1 $CD8^+$ T cell lytic activity against B16OVA target cells in vitro according to the manufacturer's guidelines. B16OVA cells were cultured in cRPMI with Geneticin G418 (1 mg/ml). After confluence, cells were dissociated using trypsin EDTA (Invitrogen, Carlsbad, CA). A total of 10^4 target cells were incubated with serially diluted, previously activated effector T cells in 200 μl of assay medium in a 96-well plate. After 6 hours, the plate was centrifuged at 1500 revolutions per minute, the supernatant was transferred, and 100 μl of LDH reaction mixture was added. The plate was incubated at room temperature away from light for 10 min, and absorbance was measured at 492 nm. Percent cell–mediated cytotoxicity was calculated as follows: 100 × (experimental – effector spontaneous – target spontaneous)/(target maximum – target spontaneous).

8-MOP/UVA treatment of murine and human tumor cells

To induce apoptosis, 2.5×10^6 tumor cells (B16OVA, YUCOT, YUSOC, YUSIV, HPV^- SCC61, and HPV^+ SCC61) were incubated with 8-MOP (200 ng/ml; UVADEX, Therakos) in 300 μl of FBS for 20 min and subsequently exposed to 2 J/cm^2 (B16OVA and B16F10) or 4 J/cm^2 (YUCOT, YUSOC, YUSIV, HPV^- SCC61, and HPV^+ SCC61) of UVA irradiation. 8-MOP and UVA dosages for each cell line were preestablished by titration to identify the minimal 8-MOP/UVA dose required to render tumor cells nonviable (tumor cell viability assessed by monitoring cell survival and proliferation over 10-day culture following 8-MOP/UVA exposure).

EMA cell death analysis

A stock concentration of EMA (Invitrogen) at 5 mg/ml in dimethyl sulfoxide was kept frozen and light protected. EMA was diluted in staining buffer to a concentration of 3.75 μg/ml and kept on ice and in the dark just before addition to cells. Cells are resuspended at 1×10^6 cells per 100 μl (10^7/ml) in staining buffer and an equal volume of EMA (3.75 μg/ml) is added, and the cells are mixed. Cells are kept in the dark and on ice for 3 min. While keeping the tubes on ice, any caps are removed, and the cells are then exposed to a fluorescent light source for 10 min at a 15-cm distance. Cells were then washed in staining buffer and analyzed by flow cytometry. 8-MOP/UVA-treated tumor cells (B16OVA, YUCOT, YUSOC, and YUSIV) were incubated in T25 tissue culture flasks at 2.5×10^6 cells per flask and incubated for 24, 48, and 96 hours under standard culture conditions. Individual flasks were analyzed at each time point for cell death by EMA. Untreated cells were analyzed as negative control.

Tumor cell growth assay

Tumor cells (B16OVA, YUCOT, YUSOC, and YUSIV) either untreated or treated with 8-MOP/UVA (as described above) were plated in six-well plates at multiple concentrations (1×10^4 to 5×10^5 cells per well) and imaged at 24, 48, and 96 hours after initial plating. Cells were monitored by bright-field imaging at ×10 magnification using Accu-Scope 3031 Microscope Series, and images were taken using Micrometrics SE Premium 4.

Human donor PBMC isolation

All studies were performed with blood donated by healthy HLA-A2–restricted volunteers. Written informed consent was obtained from all volunteers, and the studies were conducted in accordance with recognized ethical guidelines [e.g., Declaration of Helsinki, Council for International Organizations of Medical Sciences (CIOMS), Belmont Report, and U.S. Common Rule] and were approved by Yale Human Investigational Review Board under protocol number 0301023636. Peripheral blood was collected into 1:100 of heparin (5000 U/ml; McKesson Packaging Services) and platelet-containing PBMCs isolated by density gradient centrifugation over ISOLYMPH (CTL Scientific Supply Corp.) per the manufacturer's protocol, followed by treatment with ACK buffer (Lonza) to eliminate the residual red blood cells. All studies were performed with blood donated by healthy volunteers. We obtained written informed consent from all volunteers, and the studies were conducted in accordance with recognized ethical guidelines (e.g., Declaration of Helsinki, CIOMS, Belmont Report, and U.S. Common Rule) and were approved by Yale Human Investigational Review Board under protocol number 0301023636.

Platelet depletion (negative selection) from human PBMCs

Human CD61 MicroBeads and column magnetic separation (Miltenyi Biotec 130-051-101 and 130-042-401) were used for platelet depletion of human PBMCs. Platelet depletion confirmed by Hemavet quantification as above.

Monocyte isolation from human PBMCs

Pan Monocyte Isolation Kit, Human (Miltenyi Biotec, 130-096-537 and 130-042-401) was used for the negative selection of monocytes from human PBMCs. For preparation of platelet-depleted monocytes, human PBMCs were first incubated with huCD61 MicroBeads and then washed and treated with the using the Pan Monocyte Isolation Kit as above. Monocyte isolation purity was confirmed by flow cytometry, while platelet content was monitored by Hemavet quantification as above.

Overnight incubation of human PBMCs or monocytes with soluble and cellular antigen

Isolated human PBMCs or monocytes were cultured at 2.5×10^6 cells/ml overnight in RPMI 1640 without phenol red (Invitrogen, Carlsbad, CA) supplemented with 15% human AB serum (Lonza) or autologous donor serum, 1% penicillin/streptomycin (Invitrogen), and 1% L-glutamine (Invitrogen) under standard conditions. Soluble antigens; form-fitting peptides, MART1^{27L}, HPV E6$^{29-38}$, and HPV E7$^{11-19}$; and LPs, MART1 LP and E7 LP, were added to PBMCs or monocytes during overnight culture. For cultures with apoptotic tumors as cellular antigen, 8-MOP/UVA–treated tumor cells, YUCOT, YUSOC, YUSIV, HPV$^-$ SCC61, or HPV$^+$ SSC61, were added at 1.25×10^6 cells/ml for overnight culture. After overnight culture, cells were harvested and analyzed, or washed, and plated in 96-well plates in cRPMI supplemented with 15% human AB serum (Lonza).

Human transgenic T cells

The DMF5 HLA-A2–restricted CD8$^+$ T cells were originally derived and expanded for autologous T cell transfer therapy within the Rosenberg group, NCI Surgery Branch (gift of J. R. Wunderlich, Surgery Branch Cell Prep Core). Cell line was expanded and cryopreserved within the Edelson group in the Department of Dermatology, Yale University. HPV E6 and E7 HLA-A2–restricted CD8$^+$ T cell lines were originally clonally expanded from patient TIL and tested for reactivity against HPV-associated tumors by the Hinrichs group, NCI Clinical Research Center. E6 and E7 CD8$^+$ T cells were reproduced within the Edelson group from healthy HLA-A2$^+$ donor T cells isolated using negative selection (Miltenyi Biotec) and transduced to coexpress either the anti-E6(29-38) TCR anti-E7(11-19) TCR from viral vectors (provided by the Hinrichs group). CD8 T cells were expanded using a rapid expansion protocol. Following expansion, CD8 T cell purity was determined with flow cytometry analysis.

Human T cell activation assays

DMF5, HPV E6, and HPV E7 T cells were cocultured at 1×10^6/ml in 96-well plates with 1×10^6/ml of antigen-loaded PBMCs or 1×10^5/ml of antigen-loaded monocytes for 3 days under standard culture conditions. Coculture supernatants were analyzed for hIFNg ELISA (BioLegend no. 430103) per the manufacturer's instruction.

Human flow cytometry analysis

Cells harvested after overnight incubation were stained following standard protocols. Experiments used antibodies specific for human FcR block (BioLegend #422302), CD11c (Bu15, BioLegend #337214), CD80 (2D10, BioLegend #305220), CD86 (Bu63, BioLegend #374210) HLA-DR (L243, BioLegend #307629), HLA-A,B,C (W6/32, BioLegend #311410), CD14 (M5E2, BioLegend #301828), CD63 (H5C6, BioLegend #353007), CD61 (VI-PL2, BioLegend #336416), CD41/CD61 (PAC-1, BioLegend 362804), CD62p (AK4, BioLegend #304906), mTCRb (H57-597, BioLegend #109206), CD4 (OKT4, BioLegend #317428), CD8 (SK1, BioLegend #344704), and human CD3-APC (Clone OKT3, BioLegend). Color-matched isotype control antibodies were obtained from the same vendors. Flow cytometry was performed with a Stratedigm flow cytometer with electronic gates set on live cells by a combination of forward and side light scatter and 7-AAD (BioLegend), EMA (Invitrogen), Zombie Aqua (BioLegend), or Zombie NIR (BioLegend) exclusion. A minimum of 3×10^4 events were collected per sample, and data were analyzed with FlowJo software (FlowJo LLC).

Western blotting

Cell lysates were prepared by incubating platelet containing or platelet-deprived monocytes in 1% Triton X-100 in 10 mM tris (pH 7.4) and 150 mM sodium chloride + protease inhibitors (cOmplete Protease Inhibitor Cocktail, Roche) + phosphatase inhibitors (PhosSTOP, Roche) at 4°C for 1 hour. Protein estimation of the clarified lysate was carried out using Bradford dye (Bio-Rad). Laemmli sample buffer was added to clarified lysates containing equal amount of protein and subjected to SDS–polyacrylamide gel electrophoresis, followed by Western blotting. Antibodies used for analysis, c-Src, ATK, p-AKT, GRP94, glyceraldehyde-3-phosphate dehydrogenase (Proteintech), Phospho-Src, ERK, Phospho-ERK (Cell Signaling Technologies), anti-MART1 antibody (A103; a gift of R. Halaban), or anti-OVA monoclonal antibody (mAb) (Rockland), were used as per the supplier's recommendations.

Amnis imaging

ImageStream data and images were acquired using the Amnis Inspire software and the Amnis ImageStream^X Mk II two-camera system, using the 405, 488, 561, and 642 lasers and the 60× objective. Data were analyzed using Amnis IDEAS software (Luminex Corp.). Colocalization was determined using the similarity feature of IDEAS. Similarity feature as defined by IDEAS is as follows: the log-transformed Pearson's correlation coefficent and the measure of the degree to which two images are linearly correlated within a masked region.

Immunofluorescence imaging using confocal microscopy

Before imaging analysis, mouse or human PBMC was allowed to adhere on untreated ibidi μ-Slide VI (ibidi) overnight in media containing autologous serum. Cells were then fixed with 4% Paraformaldehyde (PFA), followed by staining with fluorophore conjugated antibodies anti-mouse CD41 (BD #562917), CD11b (M1/70, BioLegend #101254), Ly6G (1A8, BioLegend #127626), CD62P (RB40.34, BD #563674), anti-human CD61 (VI-PL2, BD #744381), CD14 (BioLegend #325630), CD162 (BD #562806), and CD62p (BioLegend #304918). For NFκB nuclear translocation analysis, platelet-containing or platelet-depleted human monocytes were incubated overnight in a Petri dish. Subsequently, cells were harvested and stained with NFκB (D14E12, Cell Signaling Technologies #8242) according to the standard protocol. For fixation and permeabilization, eBioscience FoxP3/transcription factor staining kit (Thermo Fisher Scientific 00-5523-00) was used. After staining procedure, cells were transferred on to ibidi μ-Slide for confocal visualization. Mean intensity

of NFκB signal was measured within the 4′,6-diamidino-2-phenylindole (DAPI)–stained nuclei of $CD14^+$ monocytes. Fluorescent images were obtained using spinning disk confocal microscope, using an UltraVIEW VoX System (PerkinElmer) equipped with 405-, 488-, 561-, and 647-nm solid-state lasers (Melles Griot), 60× 1.4–numerical aperture oil objective lens, and 1 kb × 1 kb electron multiplying charge-coupled device (Hamamatsu Photonics), and controlled by Volocity software.

Calcium influx analysis

Ca^{++} influx was determined by using Fluo-4 Calcium Imaging Kit (Thermo Fisher Scientific), followed by costaining with anti-human CD61 antibody (Alexa Fluor 647 conjugate, BioLegend). After completing the staining protocol, cells were plated onto untreated ibidi µ-Slide (ibidi) immediately before confocal visualization and then monitored for calcium signaling. Imaging commenced upon initial focusing, and individual cells were tracked in 12-s intervals for 1 hour. Ionomycin (Thermo Fisher Scientific) addition was performed at 50 µM final concentration and imaged until signal reached saturation. Movie creation and data analysis were performed using Volocity software.

Statistics

Statistical significance in comparisons was calculated using the one-way or two-way analysis of variance (ANOVA).

SUPPLEMENTARY MATERIALS

Supplementary material for this article is available at http://advances.sciencemag.org/cgi/content/full/6/11/eaaz1580/DC1

Fig. S1. Platelet depletion from PBMCs.
Fig. S2. PBMC-driven OT1 T cell response is antigen specific and platelet dependent.
Fig. S3. Monocytes are key PBMC population necessary in observed platelet-dependent cross-presentation.
Fig. S4. Platelet-induced maturation in PBMC monocytes and cross-primed T cells.
Fig. S5. Platelet-matured monocytes demonstrate specific enhancement of antigen cross-presentation.
Fig. S6. Effect of platelet inhibitors on platelet-initiated cross-presentation.
Fig. S7. P- and E-selectin rescue cross-presentation in platelet-depleted PBMCs.
Fig. S8. rP-selectin and anti-PSGL1 mAb exhibit titratable, monocyte-specific agonist activity for initiating cross-presentation.
Fig. S9. Confocal microscopy of human monocytes in presence or absence of activated platelets.
Fig. S10. Comparison of APCs in processing apoptotic tumor cells for antigen-specific T cell proliferation.
Movie S1. 3D reconstruction of murine monocyte with platelets.
Movie S2. 3D reconstruction of human monocyte with platelets.
Movie S3. Calcium flux in human monocyte upon interaction with platelets.
Movie S4. Calcium flux is absent in human monocyte without platelet.
Movie S5. Calcium flux in human monocyte upon ionomycin stimulation.
Movie S6. 3D construction of monocyte PSGL1 expression and distribution.
Movie S7. 3D reconstruction of monocyte PSGL1 around unactivated platelet.
Movie S8. 3D reconstruction of monocyte PSGL1 around activated platelet.
Movie S9. Cross-sections of P-selectin:PSGL1 platelet-monocyte "adhesion synapse".

View/request a protocol for this paper from *Bio-protocol*.

REFERENCES AND NOTES

1. R. M. Steinman, Decisions about dendritic cells: Past, present, and future. *Annu. Rev. Immunol.* **30**, 1–22 (2012).
2. L. Bone, L. F. Whyte, S. A. Carnoutsos, A. H. Cook, D. N. Hart, Monitoring human blood dendritic cell numbers in normal individuals and in stem cell transplantation. *Blood* **93**, 728–736 (1999).
3. F. Sallusto, A. Lanzavecchia, Efficient presentation of soluble antigen by cultured human dendritic cells is maintained by granulocyte/macrophage colony-stimulating factor plus interleukin 4 and downregulated by tumor necrosis factor alpha. *J. Exp. Med.* **179**, 1109–1118 (1994).
4. M. Collin, V. Bigley, Human dendritic cell subsets: An update. *Immunology* **154**, 3–20 (2018).
5. A.-C. Villani, R. Satija, G. Reynolds, S. Sarkizova, K. Shekhar, J. Fletcher, M. Griesbeck, A. Butler, S. Zheng, S. Lazo, L. Jardine, D. Dixon, E. Stephenson, E. Nilsson, I. Grundberg, D. McDonald, A. Filby, W. Li, P. L. De Jager, O. Rozenblatt-Rosen, A. A. Lane, M. Haniffa, A. Regev, N. Hacohen, Single-cell RNA-seq reveals new types of human blood dendritic cells, monocytes, and progenitors. *Science* **356**, eaah4573 (2017).
6. Y. Osugi, S. Vuckovic, D. N. J. Hart, Myeloid blood $CD11c^+$ dendritic cells and monocyte-derived dendritic cells differ in their ability to stimulate T lymphocytes. *Blood* **100**, 2858–2866 (2002).
7. P. Kalinski, H. Edington, H. J. Zeh, H. Okada, L. H. Butterfield, J. M. Kirkwood, D. L. Bartlett, Dendritic cells in cancer immunotherapy: Vaccines or autologous transplants? *Immunol. Res.* **50**, 235–247 (2011).
8. P. J. Tacken, I. J. M. de Vries, R. Torensma, C. G. Figdor, Dendritic-cell immunotherapy: From ex vivo loading to in vivo targeting. *Nat. Rev. Immunol.* **7**, 790 (2007).
9. R. M. Steinman, I. Mellman, Immunotherapy: Bewitched, bothered, and bewildered no more. *Science* **305**, 197–200 (2004).
10. A. Langenkamp, M. Messi, A. Lanzavecchia, F. Sallusto, Kinetics of dendritic cell activation: Impact on priming of T_H1, T_H2 and nonpolarized T cells. *Nat. Immunol.* **1**, 311–316 (2000).
11. P. B. Watchmaker, E. Berk, R. Muthuswamy, R. B. Mailliard, J. A. Urban, J. M. Kirkwood, P. Kalinski, Independent regulation of chemokine responsiveness and cytolytic function versus $CD8^+$ T cell expansion by dendritic cells. *J. Immunol.* **184**, 591–597 (2010).
12. C. Cheong, I. Matos, J.-H. Choi, D. B. Dandamudi, E. Shrestha, M. P. Longhi, K. L. Jeffrey, R. M. Anthony, C. Kluger, G. Nchinda, H. Koh, A. Rodriguez, J. Idoyaga, M. Pack, K. Velinzon, C. G. Park, R. M. Steinman, Microbial stimulation fully differentiates monocytes to DC-SIGN/$CD209^+$ dendritic cells for immune T cell areas. *Cell* **143**, 416–429 (2010).
13. M. Greter, J. Helft, A. Chow, D. Hashimoto, A. Mortha, J. Agudo-Cantero, M. Bogunovic, E. L. Gautier, J. Miller, M. Leboeuf, G. Lu, C. Aloman, B. D. Brown, J. W. Pollard, H. Xiong, G. J. Randolph, J. E. Chipuk, P. S. Frenette, M. Merad, GM-CSF controls nonlymphoid tissue dendritic cell homeostasis but is dispensable for the differentiation of inflammatory dendritic cells. *Immunity* **36**, 1031–1046 (2012).
14. G. J. Randolph, S. Beaulieu, S. Lebecque, R. M. Steinman, W. A. Muller, Differentiation of monocytes into dendritic cells in a model of transendothelial trafficking. *Science* **282**, 480–484 (1998).
15. G. Zuchtriegel, B. Uhl, D. Puhr-Westerheide, M. Pörnbacher, K. Lauber, F. Krombach, C. A. Reichel, Platelets guide leukocytes to their sites of extravasation. *PLOS Biol.* **14**, e1002459 (2016).
16. A. Ventura, A. Vassall, E. Robinson, R. Filler, D. Hanlon, K. Meeth, H. Ezaldein, M. Girardi, O. Sobolev, M. W. Bosenberg, R. L. Edelson, Extracorporeal photochemotherapy drives monocyte-to-dendritic cell maturation to induce anticancer immunity. *Cancer Res.* **78**, 4045–4058 (2018).
17. J. S. Raval, N. R. Ratcliffe, Extracorporeal photopheresis and personalized medicine in the 21st century: The future's so bright! *J. Clin. Apher.* **33**, 461–463 (2018).
18. N. Kibbi, O. Sobolev, M. Girardi, R. L. Edelson, Induction of anti-tumor CD8 T cell responses by experimental ECP-induced human dendritic antigen presenting cells. *Transfus. Apher. Sci.* **55**, 146–152 (2016).
19. C. N. Morrell, A. A. Aggrey, L. M. Chapman, K. L. Modjeski, Emerging roles for platelets as immune and inflammatory cells. *Blood* **123**, 2759–2767 (2014).
20. S. Kossmann, J. Lagrange, S. Jäckel, K. Jurk, M. Ehlken, T. Schönfelder, Y. Weihert, M. Knorr, M. Brandt, N. Xia, H. Li, A. Daiber, M. Oelze, C. Reinhardt, K. Lackner, A. Gruber, B. Monia, S. H. Karbach, U. Walter, Z. M. Ruggeri, T. Renné, W. Ruf, T. Münzel, P. Wenzel, Platelet-localized FXI promotes a vascular coagulation-inflammatory circuit in arterial hypertension. *Sci. Transl. Med.* **9**, 1–17 (2017).
21. S. Rachidi, A. Metelli, B. Riesenberg, B. X. Wu, M. H. Nelson, C. Wallace, C. M. Paulos, M. P. Rubinstein, E. Garrett-Mayer, M. Hennig, D. W. Bearden, Y. Yang, B. Liu, Z. Li, Platelets subvert T cell immunity against cancer via GARP-TGFβ axis. *Sci. Immunol.* **2**, eaai7911 (2017).
22. S. C. Pitchford, S. Momi, S. Giannini, L. Casali, D. Spina, C. P. Page, P. Gresele, Platelet P-selectin is required for pulmonary eosinophil and lymphocyte recruitment in a murine model of allergic inflammation. *Blood* **105**, 2074–2081 (2005).
23. C. J. Kuckleburg, C. M. Yates, N. Kalia, Y. Zhao, G. B. Nash, S. P. Watson, G. E. Rainger, Endothelial cell-borne platelet bridges selectively recruit monocytes in human and mouse models of vascular inflammation. *Cardiovasc. Res.* **91**, 134–141 (2011).
24. M. R. Yeaman, Platelets: At the nexus of antimicrobial defence. *Nat. Rev. Microbiol.* **12**, 426–437 (2014).
25. D. R. Tough, S. Sun, X. Zhang, J. Sprent, Stimulation of naive and memory T cells by cytokines. *Immunol. Rev.* **170**, 39–47 (1999).
26. L. M. Chapman, A. A. Aggrey, D. J. Field, K. Srivastava, S. Ture, K. Yui, D. J. Topham, W. M. Baldwin III, C. N. Morrell, Platelets present antigen in the context of MHC class I. *J. Immunol.* **189**, 916–923 (2012).

27. C. Hespel, M. Moser, Role of inflammatory dendritic cells in innate and adaptive immunity. *Eur. J. Immunol.* **42**, 2535–2543 (2012).
28. G. J. Randolph, C. Jakubzick, C. Qu, Antigen presentation by monocytes and monocyte-derived cells. *Curr. Opin. Immunol.* **20**, 52–60 (2008).
29. O. P. Joffre, E. Segura, A. Savina, S. Amigorena, Cross-presentation by dendritic cells. *Nat. Rev. Immunol.* **12**, 557–569 (2012).
30. F. Geissmann, M. G. Manz, S. Jung, M. H. Sieweke, M. Merad, K. Ley, Development of monocytes, macrophages, and dendritic cells. *Science* **327**, 656–661 (2010).
31. S. R. Larson, S. M. Atif, S. L. Gibbings, S. M. Thomas, M. G. Prabagar, T. Danhorn, S. M. Leach, P. M. Henson, C. V. Jakubzick, Ly6C$^+$ monocyte efferocytosis and cross-presentation of cell-associated antigens. *Cell Death Differ.* **23**, 997–1003 (2016).
32. G. J. Randolph, K. Inaba, D. F. Robbiani, R. M. Steinman, W. A. Muller, Differentiation of phagocytic monocytes into lymph node dendritic cells in vivo. *Immunity* **11**, 753–761 (1999).
33. S. D. Wright, R. A. Ramos, P. S. Tobias, R. J. Ulevitch, J. C. Mathison, CD14, a receptor for complexes of lipopolysaccharide (LPS) and LPS binding protein. *Science* **249**, 1431–1433 (1990).
34. G. Passacquale, P. Vamadevan, L. Pereira, C. Hamid, V. Corrigall, A. Ferro, Monocyte-platelet interaction induces a pro-inflammatory phenotype in circulating monocytes. *PLOS ONE* **6**, e25595 (2011).
35. R. Goncalves, X. Zhang, H. Cohen, A. Debrabant, D. M. Mosser, Platelet activation attracts a subpopulation of effector monocytes to sites of *Leishmania major* infection. *J. Exp. Med.* **208**, 1253–1265 (2011).
36. I. Fricke, D. Mitchell, F. Petersen, A. Böhle, S. Bulfone-Paus, S. Brandau, Platelet factor 4 in conjunction with IL-4 directs differentiation of human monocytes into specialized antigen-presenting cells. *FASEB J.* **18**, 1588–1590 (2004).
37. M. Hagihara, A. Higuchi, N. Tamura, Y. Ueda, K. Hirabayashi, Y. Ikeda, S. Kato, S. Sakamoto, T. Hotta, S. Handa, S. Goto, Platelets, after exposure to a high shear stress, induce IL-10-producing, mature dendritic cells in vitro. *J. Immunol.* **172**, 5297–5303 (2004).
38. B. D. Elzey, J. Tian, R. J. Jensen, A. K. Swanson, J. R. Lees, S. R. Lentz, C. S. Stein, B. Nieswandt, Y. Wang, B. L. Davidson, T. L. Ratliff, Platelet-mediated modulation of adaptive immunity. A communication link between innate and adaptive immune compartments. *Immunity* **19**, 9–19 (2003).
39. B. S. Coller, Platelets and thrombolytic therapy. *N. Engl. J. Med.* **322**, 33–42 (1990).
40. H. Beutier, B. Hechler, O. Godon, Y. Wang, C. M. Gillis, L. de Chaisemartin, A. Gouel-Chéron, S. Magnenat, L. E. Macdonald, A. J. Murphy; NASA Study Group, S. Chollet-Martin, D. Longrois, C. Gachet, P. Bruhns, F. Jönsson, Platelets expressing IgG receptor FcγRIIA/CD32A determine the severity of experimental anaphylaxis. *Sci. Immunol.* **3**, eaan5997 (2018).
41. J. E. Freedman, J. Loscalzo, Platelet-monocyte aggregates: Bridging thrombosis and inflammation. *Circulation* **105**, 2130–2132 (2002).
42. D. A. Carlow, K. Gossens, S. Naus, K. M. Veerman, W. Seo, H. J. Ziltener, PSGL-1 function in immunity and steady state homeostasis. *Immunol. Rev.* **230**, 75–96 (2009).
43. A. Zufferey, D. Schvartz, S. Nolli, J.-L. Reny, J.-C. Sanchez, P. Fontana, Characterization of the platelet granule proteome: Evidence of the presence of MHC1 in alpha-granules. *J. Proteomics* **101**, 130–140 (2014).
44. E. M. Golebiewska, A. W. Poole, Platelet secretion: From haemostasis to wound healing and beyond. *Blood Rev.* **29**, 153–162 (2015).
45. J. W. Semple, J. E. Italiano Jr., J. Freedman, Platelets and the immune continuum. *Nat. Rev. Immunol.* **11**, 264–274 (2011).
46. P. André, P-selectin in haemostasis. *Br. J. Haematol.* **126**, 298–306 (2004).
47. Y. D. Wijeyeratne, S. Heptinstall, Anti-platelet therapy: ADP receptor antagonists. *Br. J. Clin. Pharmacol.* **72**, 647–657 (2011).
48. C. E. Green, D. N. Pearson, R. T. Camphausen, D. E. Staunton, S. I. Simon, Shear-dependent capping of L-selectin and P-selectin glycoprotein ligand 1 by E-selectin signals activation of high-avidity β_2-integrin on neutrophils. *J. Immunol.* **172**, 7780–7790 (2004).
49. R. Tinoco, D. C. Otero, A. A. Takahashi, L. M. Bradley, PSGL-1: A new player in the immune checkpoint landscape. *Trends Immunol.* **38**, 323–335 (2017).
50. K. C. Ahn, A. J. Jun, P. Pawar, S. Jadhav, S. Napier, O. J. T. McCarty, K. Konstantopoulos, Preferential binding of platelets to monocytes over neutrophils under flow. *Biochem. Biophys. Res. Commun.* **329**, 345–355 (2005).
51. L. A. Johnson, B. Heemskerk, D. J. Powell Jr., C. J. Cohen, R. A. Morgan, M. E. Dudley, P. F. Robbins, S. A. Rosenberg, Gene transfer of tumor-reactive TCR confers both high avidity and tumor reactivity to nonreactive peripheral blood mononuclear cells and tumor-infiltrating lymphocytes. *J. Immunol.* **177**, 6548–6559 (2006).
52. L. M. Draper, M. L. M. Kwong, A. Gros, S. Stevanovi, E. Tran, S. Kerkar, M. Raffeld, S. A. Rosenberg, C. S. Hinrichs, Targeting of HPV-16$^+$ epithelial cancer cells by TCR gene engineered T cells directed against E6. *Clin. Cancer Res.* **21**, 4431–4439 (2015).
53. I. Zanoni, R. Ostuni, G. Capuano, M. Collini, M. Caccia, A. E. Ronchi, M. Rocchetti, F. Mingozzi, M. Foti, G. Chirico, B. Costa, A. Zaza, P. Ricciardi-Castagnoli, F. Granucci, CD14 regulates the dendritic cell life cycle after LPS exposure through NFAT activation. *Nature* **460**, 264–268 (2009).
54. P. Piccardoni, R. Sideri, S. Manarini, A. Piccoli, N. Martelli, G. de Gaetano, C. Cerletti, V. Evangelista, Platelet/polymorphonuclear leukocyte adhesion: A new role for SRC kinases in Mac-1 adhesive function triggered by P-selectin. *Blood* **98**, 108–116 (2001).
55. H.-B. Wang, J.-T. Wang, L. Zhang, Z. H. Geng, W.-L. Xu, T. Xu, Y. Huo, X. Zhu, E. F. Plow, M. Chen, J.-G. Geng, P-selectin primes leukocyte integrin activation during inflammation. *Nat. Immunol.* **8**, 882–892 (2007).
56. T. Xu, L. Zhang, Z. H. Geng, H.-B. Wang, J.-T. Wang, M. Chen, J.-G. Geng, P-selectin cross-links PSGL-1 and enhances neutrophil adhesion to fibrinogen and ICAM-1 in a Src kinase-dependent, but GPCR-independent mechanism. *Cell Adh. Migr.* **1**, 115–123 (2007).
57. H. Mueller, A. Stadtmann, H. van Aken, E. Hirsch, D. Wang, K. Ley, A. Zarbock, Tyrosine kinase Btk regulates E-selectin-mediated integrin activation and neutrophil recruitment by controlling phospholipase C (PLC) γ2 and PI3Kγ pathways. *Blood* **115**, 3118–3127 (2010).
58. A. S. Weyrich, T. M. McIntyre, R. P. McEver, S. M. Prescott, G. A. Zimmerman, Monocyte tethering by P-selectin regulates monocyte chemotactic protein-1 and tumor necrosis factor-alpha secretion. Signal integration and NF-kappa B translocation. *J. Clin. Invest.* **95**, 2297–2303 (1995).
59. K. I.-P. J. Hidari, A. S. Weyrich, G. A. Zimmerman, R. P. McEver, Engagement of P-selectin glycoprotein ligand-1 enhances tyrosine phosphorylation and activates mitogen-activated protein kinases in human neutrophils. *J. Biol. Chem.* **272**, 28750–28756 (1997).
60. J. Xie, J. Qian, J. Yang, S. Wang, M. E. Freeman III, Q. Yi, Critical roles of Raf/MEK/ERK and PI3K/AKT signaling and inactivation of p38 MAP kinase in the differentiation and survival of monocyte-derived immature dendritic cells. *Exp. Hematol.* **33**, 564–572 (2005).
61. L. E. Rameh, L. C. Cantley, The role of phosphoinositide 3-kinase lipid products in cell function. *J. Biol. Chem.* **274**, 8347–8350 (1999).
62. D. J. Rawlings, A. M. Scharenberg, H. Park, M. I. Wahl, S. Lin, R. M. Kato, A.-C. Fluckiger, O. N. Witte, J.-P. Kinet, Activation of BTK by a phosphorylation mechanism initiated by SRC family kinases. *Science* **271**, 822–825 (1996).
63. S. Vijayan, T. Sidiq, S. Yousuf, P. J. van den Elsen, K. S. Kobayashi, Class I transactivator, NLRC5: A central player in the MHC class I pathway and cancer immune surveillance. *Immunogenetics* **71**, 273–282 (2019).
64. R. R. Brutkiewicz, Cell signaling pathways that regulate antigen presentation. *J. Immunol.* **197**, 2971–2979 (2016).
65. A. S. Weyrich, M. R. Elstad, R. P. McEver, T. M. McIntyre, K. L. Moore, J. H. Morrissey, S. M. Prescott, G. A. Zimmerman, Activated platelets signal chemokine synthesis by human monocytes. *J. Clin. Invest.* **97**, 1525–1534 (1996).
66. R. L. Edelson, Mechanistic insights into extracorporeal photochemotherapy: Efficient induction of monocyte-to-dendritic cell maturation. *Transfus. Apher. Sci.* **50**, 322–329 (2014).
67. K. Tatsuno, T. Yamazaki, D. Hanlon, P. Han, E. Robinson, O. Sobolev, A. Yurter, F. Rivera-Molina, N. Arshad, R. L. Edelson, L. Galluzzi, Extracorporeal photochemotherapy induces bona fide immunogenic cell death. *Cell Death Dis.* **10**, 578 (2019).
68. M. Krauthammer, Y. Kong, B. H. Ha, P. Evans, A. Bacchiocchi, J. P. McCusker, E. Cheng, M. J. Davis, G. Goh, M. Choi, S. Ariyan, D. Narayan, K. Dutton-Regester, A. Capatana, E. C. Holman, M. Bosenberg, M. Sznol, H. M. Kluger, D. E. Brash, D. F. Stern, M. A. Materin, R. S. Lo, S. Mane, S. Ma, K. K. Kidd, N. K. Hayward, R. P. Lifton, J. Schlessinger, T. J. Boggon, R. Halaban, Exome sequencing identifies recurrent somatic RAC1 mutations in melanoma. *Nat. Genet.* **44**, 1006–1014 (2012).
69. J. E. Grotzke, D. Sengupta, Q. Lu, P. Cresswell, The ongoing saga of the mechanism (s) of MHC class I-restricted cross-presentation. *Curr. Opin. Immunol.* **46**, 89–96 (2017).
70. E. Gubanova, B. Brown, S. V. Ivanov, T. Helleday, G. B. Mills, W. G. Yarbrough, N. Issaeva, Downregulation of SMG-1 in HPV-positive head and neck squamous cell carcinoma due to promoter hypermethylation correlates with improved survival. *Clin. Cancer Res.* **18**, 1257–1267 (2012).
71. A. Grakoui, S. K. Bromley, C. Sumen, M. M. Davis, A. S. Shaw, P. M. Allen, M. L. Dustin, The immunological synapse: A molecular machine controlling T cell activation. *Science* **285**, 221–227 (1999).
72. K.-H. Lee, A. R. Dinner, C. Tu, G. Campi, S. Raychaudhuri, R. Varma, T. N. Sims, W. R. Burack, H. Wu, J. Wang, O. Kanagawa, M. Markiewicz, P. M. Allen, M. L. Dustin, A. K. Chakraborty, A. S. Shaw, The immunological synapse balances T cell receptor signaling and degradation. *Science* **302**, 1218–1222 (2003).
73. J.-E. Alard, A. Ortega-Gomez, K. Wichapong, D. Bongiovanni, M. Horckmans, R. T. A. Megens, G. Leoni, B. Ferraro, J. Rossaint, N. Paulin, J. Ng, H. Ippel, D. Suylen, R. Hinkel, X. Blanchet, F. Gaillard, M. D'Amico, P. von Hundelshausen, A. Zarbock, C. Scheiermann, T. M. Hackeng, S. Steffens, C. Kupatt, G. A. F. Nicolaes, C. Weber, O. Soehnlein, Recruitment of classical monocytes can be inhibited by disturbing heteromers of neutrophil HNP1 and platelet CCL5. *Sci. Transl. Med.* **7**, 317ra196 (2015).
74. M. Le Borgne, N. Etchart, A. Goubier, S. A. Lira, J. C. Sirard, N. Rooijen, C. Caux, S. Aït-Yahia, A. Vicari, D. Kaiserlian, B. Dubois, Dendritic cells rapidly recruited into epithelial tissues via

CCR6/CCL20 are responsible for $CD8^+$ T cell crosspriming in vivo. *Immunity* **24**, 191–201 (2006).
75. C. S. K. Ho, D. Munster, C. M. Pyke, D. N. J. Hart, J. A. López, Spontaneous generation and survival of blood dendritic cells in mononuclear cell culture without exogenous cytokines. *Blood* **99**, 2897–2904 (2002).
76. T. S. Durazzo, R. E. Tigelaar, R. Filler, A. Hayday, M. Girardi, R. L. Edelson, Induction of monocyte-to-dendritic cell maturation by extracorporeal photochemotherapy: Initiation via direct platelet signaling. *Transfus. Apher. Sci.* **50**, 370–378 (2014).

Acknowledgments: We thank M. Ene for guiding discussions, critical inputs, and unwavering intellectual support throughout project development, manuscript preparation, and visual media curation. We thank B. Coller at Rockefeller University and P. Cresswell in the Department of Immunobiology at Yale School of Medicine for formative discussions and manuscript review. We thank R. Flavell and K. Herold in the Department of Immunobiology at Yale School of Medicine for helpful discussions. We also thank D. Horwitz at University of Southern California school of Rheumatology for intellectual discussions. I. Mellman (Genentech) was an early intellectual force in this work, and we thank him for years of open-mindedness and early guidance regarding the setup of mouse models, optimal experiments for assessing antigen presentation, and processing in DCs. We thank our volunteer blood donors and I. Christensen and her staff at Yale ECP Treatment Center for help with volunteer blood procurement. **Funding:** Given the general implications of the findings for cell therapy, partial funding was facilitated by Integraid Inc. (for partial funding P.H. in the Fahmy Lab) and Toralgen Inc. for procurement of reagents in this work. Partial funding for effort in the Fahmy Lab was also provided by NIH 1R01CA026412, NSF Graduate Research Fellowship Program (to P.H.) and discretionary funds from the Fahmy Lab. Additional funding for the work was provided by Yale Cancer Center (R.E.), NY Cardiac Center GS056321 (R.E.), NIAMSD Training Grant 5T32AR007016, as well as NIH R01- AI097206 (by P. Cresswell), Cancer Research Institute Irvington Postdoctoral Fellowship (to N.A.), and NIH R01GM118486 (to D.T.). **Author contributions:** P.H. conceptualized and designed the research, curated data, performed experiments, analyzed the results, and drafted the manuscript. D.H. also designed research and methodology, performed experiments, and drafted the manuscript. N.A. performed investigation and drafted the manuscript. J.S.L. and K.T. performed investigation, data curation, analysis, and manuscript revision. C.C. and F.R.-M. performed investigation. E.R. performed project administration and resource management. R.F. performed experiments and provided resources. O.S. discussed the results, helped with visualization, and drafted the manuscript. D.T. provided funding and resources. T.F. and R.E. conceptualized the research, acquired funding, and provided project supervision. **Competing interests:** O.S. is VP Immunology at Transimmune AG. R.E. has ownership interest (including patents) in and is a consultant/advisory board member of Transimmune AG. All other authors declare that they have no competing interests. **Data and materials availability:** All data needed to evaluate the conclusions in the paper are present in the paper and/or the Supplementary Materials. Additional data related to this to this paper may be requested from the authors. The human DMF5 cell line can be provided by the Surgery Branch, NCI, pending scientific review and a completed material transfer agreement. Requests for the DMF5 cell line should be submitted to S. Rosenberg, MD, PhD, Surgery Branch, NCI.

Submitted 16 August 2019
Accepted 17 December 2019
Published 11 March 2020
10.1126/sciadv.aaz1580

Citation: P. Han, D. Hanlon, N. Arshad, J. S. Lee, K. Tatsuno, E. Robinson, R. Filler, O. Sobolev, C. Cote, F. Rivera-Molina, D. Toomre, T. Fahmy, R. Edelson, Platelet P-selectin initiates cross-presentation and dendritic cell differentiation in blood monocytes. *Sci. Adv.* **6**, eaaz1580 (2020).